TECHNOECONOMIC ASSESSMENT OF PVT-INTEGRATED HEAT PUMP SYSTEM WITH THERMAL ENERGY STORAGE FOR RESIDENTIAL APPLICATIONS

A Thesis Submitted to
the Graduate School of
İzmir Institute of Technology
in Partial Fulfillment of the Requirements for the Degree of

MASTER OF SCIENCE
in Energy Engineering

by
Ümran Özge ÇAĞIRIR

September 2025
İZMİR

We approve the thesis of **Ümran Özge ÇAĞIRIR**

Examining Committee Members:

Assoc. Prof. Dr. Başar ÇAĞLAR
Department of Energy Engineering, Izmir Institute of Technology

Assoc. Prof. Dr. Haktan KARADENİZ
Department of Energy Engineering, Izmir Institute of Technology

Prof. Dr. Nurdan YILDIRIM
Department of Mechanical Engineering, Yaşar University

19 September 2025

Assoc. Prof. Dr. Başar ÇAĞLAR
Supervisor, Department of
Energy Engineering,
İzmir Institute of Technology

Prof. Dr. Mousa MOHAMMADPOURFARD
Co-Supervisor, Department of
Energy Engineering, İzmir Institute of
Technology

Prof. Dr. Gülden Gökçen AKKURT
Head of the Department of
Energy Engineering,
İzmir Institute of Technology

Prof. Dr. Mehtap EANES
Dean of the Graduate School

ACKNOWLEDGEMENTS

I would like to express my sincere gratitude to my supervisor, Assoc. Prof. Dr. Başar ÇAĞLAR, for her continuous guidance, valuable insights, and encouragement throughout this study.

I am also thankful to my co-advisor, Prof. Dr. Mousa MOHAMMADPOURFARD for her constructive feedback, support, and motivation that enriched both the research process and this thesis.

My special thanks go to the members of the jury committee, Prof. Dr. Nurdan YILDIRIM and Assoc. Prof. Dr. Haktan KARADENİZ for their insightful comments, suggestions, and valuable time devoted to reviewing my work.

I am deeply grateful to my parents, Nihal ŞEBİK and Mustafa ŞEBİK whose steady support carried me through this journey. I also thank my siblings Ceyda ŞEBİK, and Metin ŞEBİK for their constant encouragement and warmth.

I would like to express my heartfelt gratitude to my husband, Ertuğrul ÇAĞIRIR, whose unwavering support and understanding have been invaluable throughout this study.

I would like to express my sincere gratitude to Zeynep KAHRAMAN, Nisa YILDIRIM, Merve ÜNAL, Belka ANYA, Ece İNAN, and my colleagues in AYBU B305 for their constant motivation and support throughout this study.

ABSTRACT

TECHNOECONOMIC ASSESSMENT OF PVT INTEGRATED HEAT PUMP SYSTEM WITH THERMAL ENERGY STORAGE FOR RESIDENTIAL APPLICATIONS

Climate change and decarbonization targets foreground low-carbon residential heating solutions. This study conducts a techno-economic assessment, under Izmir's climate, of a hybrid system that combines photovoltaic-thermal (PVT) collectors, an air-source heat pump (ASHP), and phase-change-material-based thermal energy storage (PCM-TES), using a MATLAB-based model and an energy-management algorithm. Three scenarios are compared: (1) ASHP-only, (2) PVT+ASHP, and (3) PVT+TES+ASHP. The ASHP-only case is fully grid-dependent, yields a negative IRR, and an LCOH more than twice that of natural gas. Adding PVT reduces grid electricity consumption; however, its contribution to the heat load remains <20% even with 25 modules, and the overall economics remain unfavourable. With PVT+PCM, performance improves markedly: with 200 kWh of PCM and four PVT modules, the entire heat load can be met by PVT+TES; LCOH ≈ $0.091/kWh, IRR ≈ 1.2%, payback ≈ 21.5 years; and the total LCOE is 0.114 $/kWh, lower than ASHP-only (0.123 $/kWh). Sensitivity analysis indicates that outcomes are most sensitive to the PVT capital cost, PCM specific cost, and the retail electricity price, while a low feed-in tariff limits the value of surplus PV electricity. Overall, although PVT and PCM integration enhances the technical performance and self-sufficiency of ASHP systems in Mediterranean climates, such systems are not economically attractive under current Turkish market conditions. The main conclusion is that these renewable hybrid configurations only become economically viable with reductions in system costs, supportive policy incentives or optimized system design. Under such conditions, they can realistically contribute to sustainable heating strategies.

ÖZET

KONUT UYGULAMALARI İÇİN TERMAL ENERJİ DEPOLAMALI PVT ENTEGRE ISI POMPASI SİSTEMİNİN TEKNOEKONOMİK DEĞERLENDİRMESİ

İklim değişikliği ve karbonsuzlaşma hedefleri, konut ısıtmasında düşük karbonlu çözümleri öne çıkarmaktadır. Bu çalışma, İzmir koşullarında fotovoltaik-termal (PVT) kolektör, hava kaynaklı ısı pompası (ASHP) ve faz değiştiren malzemeye (PCM) dayalı ısıl depolamayı birleştiren hibrit bir sistemi MATLAB tabanlı model ve enerji yönetim algoritmasıyla tekno ekonomik olarak inceler. Üç senaryo karşılaştırılmıştır: (1) yalnız ASHP, (2) PVT+ASHP, (3) PVT+TES+ASHP. Yalnız ASHP tamamen şebekeye bağımlı, IRR negatif ve LCOH doğal gazın >2 katıdır. PVT entegrasyonu şebeke elektriğini azaltır; ancak ısı yüküne katkısı 25 modülde bile <%20 olup ekonomik açıdan olumsuz kalır. PVT+PCM ile performans belirgin artar; 200 kWh PCM ve 4 PVT'de ısı yükü bütünüyle PVT+TES ile karşılanır; LCOH ≈ 0.091 $/kWh, IRR ≈ %1.2, geri ödeme ≈ 21.5 yıl; toplam LCOE 0.114 $/kWh ile yalnız ASHP'den (0.123) düşüktür. Duyarlılık analizi, sonuçların PVT/PCM maliyetlerine ve elektrik fiyatına en hassas olduğunu; düşük alım tarifesinin fazla PV elektriğinin değerini sınırladığını gösterir. Bu bulgular, Akdeniz iklimlerinde PVT ve PCM entegrasyonunun ASHP sistemlerinin teknik performansını ve kendi kendine yeterliliğini artırmasına rağmen, sistemlerin mevcut Türkiye pazar koşullarında ekonomik olarak cazip olmadığını göstermektedir. Ana sonuç, bu tür hibrit konfigürasyonların ekonomik olarak uygun hale gelebilmesi için sistem maliyet azaltımları, politika teşvikleri veya optimize edilmiş sistem tasarımı gerektirdiği ve bu koşullar sağlandığında uzun vadeli sürdürülebilir ısıtma stratejilerine gerçekçi bir katkı sunabileceğidir.

TABLE OF CONTENTS

LIST OF FIGURES

Figure **Page**

LIST OF TABLES

Table **Page**

CHAPTER 1

INTRODUCTION

The Paris Agreement indicates that global warming over 1.5°C may result in droughts and extreme weather events (UNFCCC 2015, 2). To reduce global warming to 1.5°C, greenhouse gas emissions must be reduced by 43% by 2030 (IPCC 2023, 92). The heating sector is one of the biggest energy users in buildings worldwide and significantly contributes to the rise of greenhouse gas emissions. The International Energy Agency Report states that global demand for heating energy reached 62 exajoules in 2021, corresponding to almost 250 million tons of carbon dioxide emissions. Space heating constitutes 70% of worldwide heating demand, with natural gas fulfilling 42% of this requirement (IEA 2022, 20).

Fossil fuel-based heating systems create significant obstacles regarding environmental consequences and economic viability. In the past, before the Industrial Revolution, wood was the primary fuel source for home heating. However, over time, coal replaced wood due to increasing energy demands and the greater availability of coal. At the beginning of the 20th century, petroleum-derived gases began to replace coal for residential heating, providing more practical alternatives to coal for buildings (Zhao, McDonell, and Samuelsen 2022, 6).

However, in the 21st century, it is important to adopt more efficient and environmentally friendly alternative heating methods. The heat pump, known for its high efficiency, is a recommended technology for domestic heating. Heat pump technologies are classified according to three basic criteria: heat source and waste heat medium, the heating/cooling distribution fluid, and the thermodynamic cycle principles. On the other hand, water-to-air heat pumps use sources such as groundwater or solar-heated water to exchange heat with the environment. Water-to-water heat pumps use water as both a source and transfer medium and are widely used in central systems. Finally, ground source heat pumps exchange heat with the ground and the environment. Heat pumps can meet the heating/cooling needs of buildings by effectively using renewable energy sources (sun, water, soil) (Goldschmidt 2003,450).

Air Source Heat Pump (ASHP) systems have replaced fossil fuel boilers thanks to their simple operation, high efficiency and environmentally friendly structure. Air-to-air type heat pumps are the most common in residential applications. However, the efficiency of these systems depends on external weather conditions; for example, seasonal coefficient performance changes of up to 36% have been observed in cold climates. Although this situation emphasizes the sensitivity of ASHP systems to climatic conditions, it does not prevent them from standing out in the residential sector as a low-carbon and energy-efficient solution in general (Z. Wang et al. 2021, 935). In the study conducted by (Zhang et al. 2017, 541) energy consumption and environmental effects of air source heat pumps (ASHP) operating at low temperatures were examined in residential heating. It was concluded that these systems provide lower energy consumption and carbon emissions compared to coal-based heating systems.

Although heat pumps stand out due to their high efficiency, their ability to be considered as an environmentally sustainable solution, especially in terms of environmental sustainability, depends on supporting electricity consumption with renewable energy sources (Gaur, Fitiwi, and Curtis 2021, 2).

In the literature, due to the high electricity consumption of heat pumps, integration with PVT systems is recommended. Photovoltaic-thermal (PVT) systems are hybrid solar technologies that consist of a photovoltaic module and thermal collector and produce both energy and heat.

According to study, photovoltaic thermal (PVT) collectors can be classified according to various criteria such as design geometry, type of application, heat transfer fluid and integration method (Islam et al. 2016, 201). When examined in terms of geometrical structure, flat plate PVTs are the most common due to their efficiency at low temperatures, whereas concentrator PVTs (CPVTs) can achieve higher thermal and electrical outputs at high irradiance. PVT systems can be used independently or integrated into movable systems depending on the purpose of use. They are also divided into two groups as liquid-based or air-based according to the fluid used. PVT systems with liquid-based fluids can generally be more efficient than air-based systems. PVT systems increase total energy consumption by using excess heat from solar panels. These systems are suitable for residential and industrial applications. PVT systems increase total energy consumption by utilizing excess heat from solar panels. These systems are suitable for residential and industrial applications solar panels. These systems are suitable for residential and industrial applications.

However, especially for residential heating, insufficient solar radiation during the winter months, despite the increasing heating demand at night, causes a mismatch between energy production and consumption. This situation reduces both the economic and energy performance of the system. To overcome this problem, thermal energy storage solutions are considered as an effective option.

Thermal energy storage (TES) systems are an effective solution for eliminating the supply-demand imbalance of renewable energy sources because they allow excess heat to be stored and used when needed. TES systems are divided into three: sensible heat (SHS), latent heat (LHS) and thermochemical methods. Sensible heat storage stores heat through temperature change and is carried out with materials such as water, stone and concrete; more compact solutions are needed due to its low energy density. Latent heat storage (LHS) systems are based on materials that can store high amounts of heat through phase change and are divided into three main groups: solid–solid, solid–liquid and liquid–gas phase changes. In solid–solid phase change, the material stores heat by changing its crystal structure; this method is rarely preferred due to its low heat transfer rate. Solid–liquid phase change is the most widely used method. In this method, a high amount of latent heat is stored during the phase change and is frequently used especially in buildings, solar energy systems and with heat pumps. Although liquid-gas phase change can store very high amounts of energy, it is limited in practical applications due to the large volume change and high-pressure requirements. Therefore, PCMs that undergo solid-liquid phase change stand out as the most suitable solution in terms of both energy density and ease of use (Cabeza et al. 2011, 1676; Nair et al. 2022, 3). Phase change materials (PCMs) are divided into three main groups according to their chemical structures: organic, inorganic and eutectic. Organic PCMs are divided into two groups: paraffin and non-paraffin; paraffins are widely used in thermal energy storage systems, while non-paraffin materials such as fatty acids stand out with their environmental friendliness and the lack of additional encapsulation (Teamah 2021, 3833).

The advantages of inorganic PCMs are that they are cheaper, non-flammable and generally consist of salt hydrates and metals, while their disadvantages are phase separation, dehydration and supercooling. Eutectic PCMs aim to reach the desired melting temperature and heat storage capacity by mixing two or more PCMs. In residential applications, PCMs are generally used in solar facades, underfloor heating systems, suspended ceilings and wall elements, reducing heating-cooling loads and contributing to energy efficiency (Bayraktar and Köse 2022, 199).

In this study, the energy and economic performance of a PCM-based thermal energy storage unit integrated into a PVT-supported Air Source Heat Pump system was analysed.

1.1 Aim and Content of the Study

This study investigates the energy and economic performance of a hybrid residential heating system consisting of a photovoltaic-thermal (PVT) collector, an air-source heat pump (ASHP), and a phase change material (PCM)-based thermal energy storage unit. The system is modelled under the climatic conditions of Izmir, Turkey, using hourly meteorological data for a full-year operation period to meet thermal and electricity load of a house with a grid inclusion. The mathematical modelling of the proposed systems was developed in MATLAB to evaluate their hourly thermal and electrical power outputs. Different scenarios were tested and their technoeconomic performances were investigated, cooling loads were excluded from the scope of this study.

The main aim of this study is to evaluate the technoeconomic performance of a photovoltaic-thermal (PVT) integrated air source heat pump system supported with phase change material (PCM)-based thermal energy storage for residential space heating as well as power supply. This is used to assess the feasibility, and cost-effectiveness of such a hybrid system under real climatic conditions. The content of the thesis is organized as follows:

- **Chapter 2** provides a review of the relevant literature.
- **Chapter 3** includes system description, climate data, component selection, system configuration.
- **Chapter 4** outlines the modelling methodology, including assumptions, data sources, and calculation procedures.
- **Chapter 5** presents the analysis results, discussion, system performance analysis, and economic evaluation.
- **Chapter 6** presents the conclusions and recommendations for future research.

CHAPTER 2

LITERATURE REVIEW

This chapter presents a comprehensive review of existing research on the technical and economic viability of HP, PVT and thermal storage containing systems for residential heating. The related literature survey was organized in a way that the studies using (i) heat pump, (ii) the combination of heat pump and PVT, (iii) the combination and heat pump, PVT and thermal storage are presented separately to analyse their individual technoeconomic performance.

2.1 Only Heat pump

Under this heading, studies focusing solely on heat pump technology to meet the heat load of residences are included. In particular, publications on the use of air source heat pumps (ASHP) in residential heating are presented; the effectiveness of these systems in meeting the annual heat load of residences under different climatic conditions is evaluated.

In the study, the energy efficiency, environmental contribution and economic advantages of heat pump systems were evaluated and a building with a useful surface of 240 m². COP values are 2.33 for heat pumps. In the economic analysis, the most advantageous system in terms of 10-year operating cost is 1903.2€ for heat pumps. The 10-year operating cost for thermal boilers with 2897.0€ for natural gas. The study reveals that heat pumps consume less energy compared to conventional fuel systems and are economically viable (Sarbu, Dan, and Sebarchievici 2014, 59).

A study evaluated the annual operating emissions and costs of air source heat pumps (ASHPs) combined with hybrid systems for residential buildings in different cities. The study was conducted for regions with high renewable energy production, such as Vancouver, Toronto, and Montreal. In cities with low electricity prices, such as Montreal, annual operating costs were reduced by 27–37%. In contrast, in cities where fossil fuel-based electricity production is dominant, such as Edmonton and Yellowknife,

the use of ASHPs increased operating costs. The COP values of the systems varied between 0.9 and 5.65 (Udovichenko and Zhong 2020, 1357).

An air source heat pump (ASHP) system integrated with direct condensing radiant panel (DRHP) for heating a 25 m² from both economic and thermodynamic perspectives. The total initial investment cost of the system was calculated as only $398.2, and the annual operating cost was $72.7 and NPV value was 107.4$. The payback period of the proposed system was found to be 7.3 years. ASHP offers lower investment cost and higher performance compared to traditional heating systems. Thermodynamically, the system COP value was found to be 2.4 (Shao et al. 2021, 14).

In the study a technical, economic and environmental analysis of the air source heat pump-supported floor heating system was performed for the heating of a three-storey villa with a heat load of 15355.98 W and a size of 362.72 m² in Denizli. As a result, the SCOP value of the heat pump was found to be 4.46 (Özçelik, Gürel, And Akdemir 2023, 45).

This study examines an air source heat pump (ASHP) system and a traditional natural gas boiler system were compared in a 2500 m² commercial building in Istanbul. According to the experimental results, the COP value of the ASHP system was measured between 3.22–4.32. The initial cost of the ASHP system was estimated at $41,500, which is higher than the $35,720 cost of the gas boiler. However, at the end of 20 years, the ASHP system offers lower life cycle costs ($130,520.56) compared to the gas boiler ($177,281.27) with a 6% energy price increase estimate (Kul and Uğural 2022, 17).

The study demonstrated that the performance of the ASHP system for residential heating was analyzed with a thermodynamic model; ASHP reduced annual primary energy consumption by 13.45% compared to coal-fired boilers. It was also determined that the COP value of the system varied between 2.2 and 3.2 depending on seasonal outdoor temperatures. These findings show that ASHP technology has high energy efficiency, especially even in low-temperature climate conditions, and offers a sustainable alternative to fossil fuel boilers in central heating applications (Zhao et al. 2023, 1)

2.2 Heat pump-PVT

This section presents studies focusing on the integration of water-based photovoltaic/thermal (PVT) collectors with air source heat pumps (ASHP) for residential space heating applications.

It was shown in the numerical study that the proposed PV/T-SAHP system significantly increased both photovoltaic and thermal performance. Compared to conventional systems, a 16.3% increase in PV efficiency and a 43% increase in COP were achieved. It was stated that the developed system is suitable for meeting the space heating needs in houses in subtropical regions. The system operates more efficiently than conventional heat pumps and solar energy systems and therefore it is emphasized that it can be a viable alternative for domestic applications (Pei et al. 2008, 978).

The authors investigated the potential to reduce energy consumption and greenhouse gas emissions by applying a solar-assisted heat pump (SAHP) system to existing Canadian residences. As a result of the annual simulations, it was found that annual energy consumption in suitable residences could be reduced by 80–90 GJ with the SAHP system. It was also stated that SAHP systems were not sufficient for the NZEB (zero energy building) target, and additional energy efficiency measures and seasonal heat storage were also required (Asaee, Ugursal, and Beausoleil-Morrison 2017, 451).

A solar PV/T–heat pump system that can provide heating, cooling, hot water and electricity generation in residential buildings throughout the year was designed and experimentally evaluated. According to the experimental findings, the COP reached 3.18 in the PV/T-supported water source heat pump (WSHP) mode, which showed superior performance compared to the conventional air source heat pump (ASHP) mode (42% higher). Under conditions where solar radiation is sufficient, the overall efficiency of the PV/T collector reached 55.4% (G. Wang et al. 2018, 935).

A system consisting of PV/T collector, heat pump and heat storage unit for heating small office buildings was evaluated for three different European cities (Rome, Milan, Krakow). In the analysis performed with hourly simulations in Matlab environment, the thermal efficiency of PV/T collectors was accepted as 60%, electrical efficiency as 15% and heat exchanger efficiency as 90%. Under these conditions, the system was able to meet 70% of the heating need in Rome, 62% in Milan and 47% in Krakow. It shows that PV/T supported heat pump systems can make a significant contribution to the heating service in regions with high solar radiation. However, it was also emphasized that additional auxiliary heating systems may be needed in cold climates (Vallati et al. 2019, 91).

The use of a hybrid system in which a PV/T panel and a heat pump are integrated for electricity generation and space heating in residences was investigated. The minimum COP value was found to be 4.2, which shows that the system operates with high

efficiency. The study emphasizes that climatic conditions play an important role in the design of PV/T-heat pump systems (Obalanlege et al. 2020,558).

A PV/T–air to water source heat pump (ASHP) system was proposed for small-scale existing buildings and annual dynamic energy simulation was performed. 10 PVT modules with dimensions of 1.012 × 1.972 m^2 were used in the study. According to the simulation results, the heating season average COP value of the system was 5.3, and the electricity generated by the PV/T module exceeded the system's consumption in April–June. The study revealed that PVT-ASHP systems, which can be implemented more easily compared to ground source heat pump (GSHP) systems, are a strong alternative in terms of energy efficiency (Bae, Chae, and Nam 2022,48).

The technical and economic analysis of a PVT-assisted heat pump system to meet the electricity and water needs of a three-bedroom flat in the UK. Scenarios were created with different numbers of PVTs (12, 20 and 24) and annual energy production and consumption were examined. As a result of the research, it was concluded that the system with 12 PVTs was the best option because its investment cost was affordable, and it met 31% of the electricity demand. The study shows that PVT-supported heat pumps are an environmentally friendly system that reduces dependency on natural gas and the grid (Obalanlege et al. 2022, 2).

An energy and economic analysis of a PV/T collector and heat pump integrated system in a three-room residence in Chengdu. According to the simulation results using TRNSYS, the electrical solar fraction in large PVT areas was up to 85%. However, for the system with optimized module area range of 27.2 m^2–34.0 m^2 for 6HP system, economic analysis concluded that the system is not profitable in Chengdu conditions due to long payback period and high LCOH (22.7-21.4 $/MWh).It was emphasized that the cost of the PVT system is not economically feasible because it is higher than the cost of grid electricity price (0.0889 $/kWh) (Bisengimana et al. 2023, 519).

The performance of a direct expansion PV/T (DX-PVT) heat pump system investigated with experimental and numerical methods for a house in Shanghai. The study determined the optimum collector area-compressor volume ratio (A/Vth) and found that as A/Vth increased, the COP value of the system increased by 61.3% and the heat gain factor (HGF) decreased by 39.6% (Liu et al. 2023, 1106).

A hybrid system of large flat plate solar collector (LFPSC) and air source heat pump (ASHP) was designed for the cold climate rural area of China and evaluated technically and economically. As a result, the average collector efficiency was found to

be 42% and COP 3.08. The payback period of the system was calculated as 6.58 years. This study presents that PVT and ASHP systems are a sustainable and clean heating solution especially in rural areas (Li et al. 2022, 1).

The optimum design and economic-ecological analysis of the integrated air source heat pump (ASHP) PVT system were conducted and validated using real building data. The building is located in Busan, Republic of Korea, and its floor area is 110 m^2. The annual heating load was determined as 5543 kWh. 10 PVTs measuring 1.012 × 1.972 m^2 were used in the study. The simulation evaluation showed that the payback period of the optimum model was 9.42 years, which was three years shorter than the conventional model. The energy consumption was reduced by 43% compared with the non-PVT model, which significantly contributed to the economic benefits and CO_2 reduction (Chae, Bae, and Nam 2023, 16).

In the study, calculated Levelized Cost of Heat (LCOH) to identify the most suitable economical solar-assisted heating system for single-family residences. In the analyses performed using the Python program, LCOH changes were examined according to different solar collector areas and heating load densities. In this study, total PVT area 13.6 m^2 was used. The lowest LCOH value was obtained with 0.28 CNY/kWh in a 120 m² residence in the air source heat pump (ASHP) + PV combination. The results show that economic optimization depends not only on climatic conditions but also on local electricity and gas prices (Herrando et al. 2023, 1).

For a single-storey house in Germany, a heat pump (HP) system integrated with PVT collectors was analysed. The examined house has a heated area of 89.1 m² and 40% of the 82.4 m² roof area is covered with PVT panels (32.9 m²). According to the simulation results, it was reported that up to 39% of the heat demand can be met with solar energy and economic viability is achieved with a positive net present value (NPV). In addition, significant increases in solar contribution and self-sufficiency rates were achieved by increasing the PVT area (Arnesson et al. 2025, 1)

Residences with PVT and HP systems were evaluated in terms of energy and economy in three cities (Athens, Thessaloniki, Kastoria) in simulations made with TRNSYS software. The results show that PV/T supported HP systems reduce energy consumption and increase grid independence. It is seen that the highest LCOH value occurs in Athens (0.077 €/kWh), which limits the economic efficiency of the PV/T system due to its low heating demand (Giama et al. 2025, 16).

2.3 Heat Pump-PVT-TES

Solar-assisted heat pump systems (serial, parallel and dual source) with a collector area of 30 m² and a maximum solar radiation of 900 W/m² were investigated both experimentally and theoretically for a building with a volume of 240 m³ in Trabzon for residential heating. In these systems, where an energy storage tank equipped with phase change material (PCM) was used, the highest seasonal performance factor (SPF) of 4.20 was obtained in the dual source system. The same system stood out as the most efficient solution by providing a net energy saving of 12,056 kWh in the season. The solar energy system alone was found to be insufficient in the cloudy climate conditions of Trabzon (Kaygusuz and Ayhan 1999, 1395).

A combined experimental and numerical evaluated the integration of an air-based PVT collector, phase change material (PCM) thermal storage unit and reverse cycle heat pump for residential buildings experimentally and numerically. Thermal-hydraulic and electrical models of PVT and PCM components were developed and experimentally validated. The study highlighted that the developed model is simple and optimized for integration into building automation systems (Fiorentini, Cooper, and Ma 2015, 32).

An experimental study analyzed the direct expansion solar integrated air source heat pump (DESIARHP) system developed with phase change materials (PCMs) and flat plate heat pipe solar regenerator in their experimental study. The system was designed to improve heating efficiency in cold climates. The system was tested in different modes based on changing solar radiation. The system was tested against different climate data. The results showed that under sunny conditions, the Solar Heat Pump mode significantly outperformed conventional ASHP systems with 72% and 100% improvements in COP and heating capacity. The study showed a dynamic payback period of 4.02 years, which is shorter than gas-fired (10.18 years) and coal-fired (12.7 years) heating methods, despite the higher initial cost of the system (Wu, Xian, and Liu 2019, 44).

A techno-economic analysis of heat-pump-integrated PV/T systems, with and without PCM, for heating a 100 m² residence in Athens during the winter months was conducted using TRNSYS. Consequently, a 40% reduction in heating load and a 42-67% decrease in electricity consumption were achieved, with PCM. The optimization process resulted in a COP value of 6.3, achieved with a collector area of 20 m² and an insulation thickness of 3 cm. In this instance, the Payback Period was determined to be 18.3 years for the PCM system and 10.2 years for the system devoid of PCM. The study revealed

that integrating PCM into solar-assisted heat pump systems reduces variable costs by 6-20% while increasing total costs by 15-20%, with the FPC + PCM configuration showing the lowest total cost among PCM integrated systems for a 20 m² collector area (Plytaria et al. 2019, 548).

A solar-assisted heat pump system operating in three modes (solar, hybrid, and heat-pump-only) was designed and experimentally investigated by developing a vacuum-tube, air-type solar collector with integrated phase-change material (PCM). As a result, thanks to PCM, the system was able to provide continuous heating for 9.5 hours even at low radiation (613 W/m²). The average COP value was 3.6, and the exergy efficiency increased by 12.1%. The system has 72.8% lower operating costs compared to electric boiler heating and the payback period of the system was calculated as 5 years. This structure is considered as a viable alternative for cold and sunny regions (Li et al. 2020, 1).

A direct expansion heat pump with a PV/T panel and embedded PCM heat storage unit for a residential heating system for high latitudes and analyzed it by simulation. Under 600W/m² sunshine, the system COP value with 20m² PV/T panel reaches 5.79, which is 70% higher than the conventional air conditioning system. The electrical, thermal and total efficiencies are calculated as 17.8%, 55.8% and 75.5%, respectively. The proposed system has a higher initial cost (¥22,000) compared to a conventional air conditioning system (¥4,500), but it offers a negative annual operating cost (–¥764), indicating savings, while the air conditioning system incurs ¥4,024/year, highlighting the proposed system's economic advantage in long-term operation (Yao et al. 2020, 279).

A system comprising a storage tank and two solar-assisted heat pumps (SAHPs) was modeled in TRNSYS for Madrid climate conditions to meet a 70 m² residence's heating load of 4278 kWh. The study evaluated two different tanks containing water and PCM were compared. The PCM tank could store 14.5% more energy in the same volume, the heating rate of the system decreased from 98.9% to 72.8% due to the long charge-discharge period. In the study, increasing the storage capacity from 1000 L to 2000 L resulted in a 1.13% increase in solar energy delivered to the heat pump ($Q_{\text{solar}} \rightarrow HP$) while the solar fraction also improves from 0.697 to 0.704, indicating a higher share of the building's heating demand met by solar energy (Belmonte et al. 2022, 1).

A PVT-supported air source heat pump (ASHP) system integrated with phase change heat storage (PCM) developed for cold climate regions. In MATLAB under different climate conditions (Lhasa, Harbin), the system COP value increased from 5.19

to 8.87 thanks to the PVT integration and a 70.91% increase in total system efficiency was achieved. For heating demand, the PV/T system supplies 20–30% while the heat pump covers 70–80%, with slight regional variations across the examined cities. The study presents the positive effect of the correct selection of phase change temperature and PVT contribution on system efficiency and the applicability of this hybrid structure to different climate regions (Gao et al. 2024, 12)

Designed for extreme hot climates, four PV/T–heat-pump configurations (PV/T-W, PV/T-PCM-W, PV/T-DXHP, PV/T-PCM-DXHP) were developed and evaluated through numerical simulations in MATLAB. In the study, energy, economic and environmental performances were compared by integrating PV/T system and phase change material. As a result, the highest performance was obtained in PV/T PCM-DXHP configuration with 12.91% electrical efficiency and 13,638 MJ annual energy production, and the system has a short payback period of 3–4 years. The NPV analysis revealed that all evaluated systems achieved positive values, indicating profitability over their lifetime, with PVT-PCM-DXHP reaching the highest NPV of ₹677,403 among the systems analyzed. The study provides important findings supporting the applicability of PVT-HP-PCM integration in sustainable buildings (Babu et al. 2024, 15627).

In the study, different hybrid system configurations were examined for the energy needs of a residence with approximately 7012 kWh/year heating, 3066 kWh/year cooling, 2400 kWh/year domestic hot water (DHW) and 4280 kWh/year electrical appliances. Using TRNSYS 17.2 software, it was shown that 96.2% self-consumption (RSC) and 86.9% self-sufficiency (DSS) were achieved in the configuration consisting of PVT collector, heat pump, thermal and electrical storage systems. It was also stated that the system offered a net present value (NPV) of €6127 over its 20-year life (Gagliano, Tina, and Aneli 2025,15).

Table 1 shows that previous studies generally focus on a single point (e.g., component-only models or economics only).

Table 1. Gap / Novelty Matrix for SAHP / PVT–HP–PCM studies

Feature / Contribution	**This thesis**	**Plytaria et al. (2019)**	**Yao et al. (2020)**	**Li et al. (2020)**	**Babu et al. (2024)**	**Gao et al. (2024)**
8760-hour dynamic energy-management (EMS)	✓	○	○	○	○	○
PVT electricity dispatched to both HP and household loads	✓	○	○	○	○	○
PCM capacity optimization	✓	△	△	△	△	△
Unified reporting of $LCOE_{el}$, $LCOH$, and IRR in one framework	✓	○	△	△	△	○
Tariff scenarios ($\boldsymbol{p_{buy}}$ / $\boldsymbol{p_{sell}}$) and sensitivity analysis	✓	○	○	○	△	○
Mediterranean residential heating context	✓	✓	○	○	○	○
Grid-independent heating configuration identified	✓	○	○	○	○	○

Legend: ✓ = present and detailed; △ = partial/limited; ○ = absent or not reported in the provided summaries.

This thesis establishes a detailed energy management system for 8760 hours and reports the results in the same framework ($LCOE_{el}$, $LCOH$, IRR, PP). It also shows the optimal range for PCM capacity and, through tariff/parity analysis, explains under what conditions a hybrid system is more economical. In short, the table summarizes the thesis's innovation: facilitating decision-making by combining hourly operation, storage sizing, and economic evaluation.

CHAPTER 3

SYSTEM DESCRIPTION

A hybrid system consisting of photovoltaic/thermal harvesters (PVT), heat pump and thermal energy storage (TES) unit was considered to meet the heating and electricity needs of a residence house located in İzmir, Turkey. A schematic representation of the system energy flow is shown in Figure 1.

As seen in Figure 1(a), there are three heat supply units: PVT collectors, TES, and heat pump for meeting the thermal load. First, the heat gained from PVT $Q_{PVTtoLoad}$ is used to meet the thermal load of the house. If there is a remaining deficit, TES $Q_{PCMtoLoad}$ and the heat pump $Q_{HPtoLoad}$ are activated sequentially to cover the additional demand. TES is charged $Q_{PCMtoLoad}$ when there is excess heat generated by PVT and discharged when the total heat supplied by PVT is not sufficient to cover the heating load. When the heat from PVT and TES is not sufficient, the heat pump operates.

As shown in Figure 1(b), electricity is supplied by two sources: PVT and the grid. The electricity generated by PVT $E_{PVTtoLoad}$ first meets the electrical load of the house. If this is insufficient, the grid provides the remaining demand $E_{gridtoLoad}$.

In Figure 1(c), when PVT-generated electricity exceeds the household demand, the surplus is directed to the grid $E_{PVTtoGrid}$. Depending on the operational scenario, a portion of the surplus electricity may also be used to power the heat pump before selling to the grid.

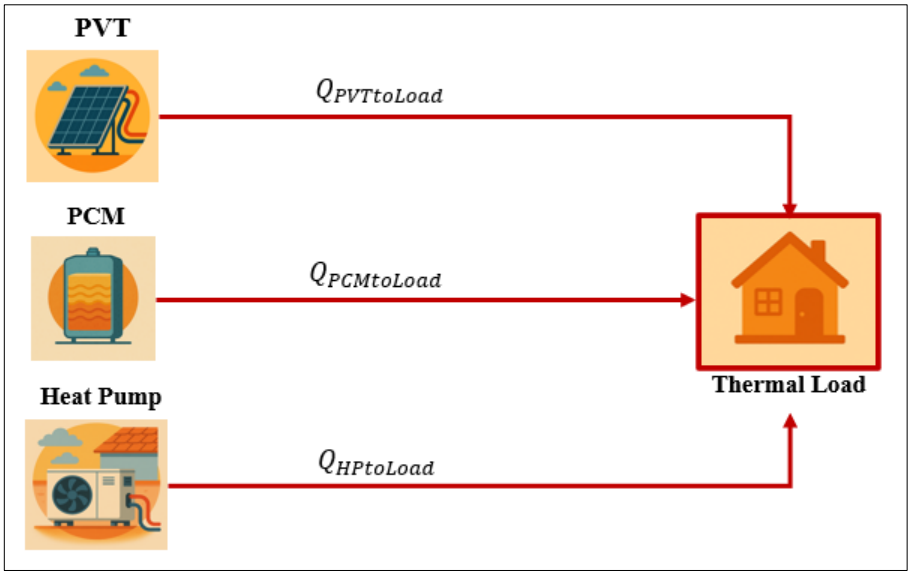

(a)

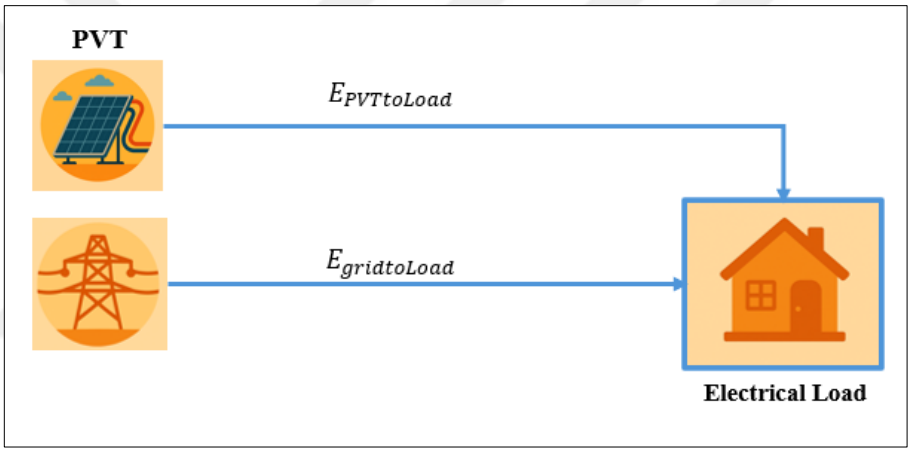

(b)

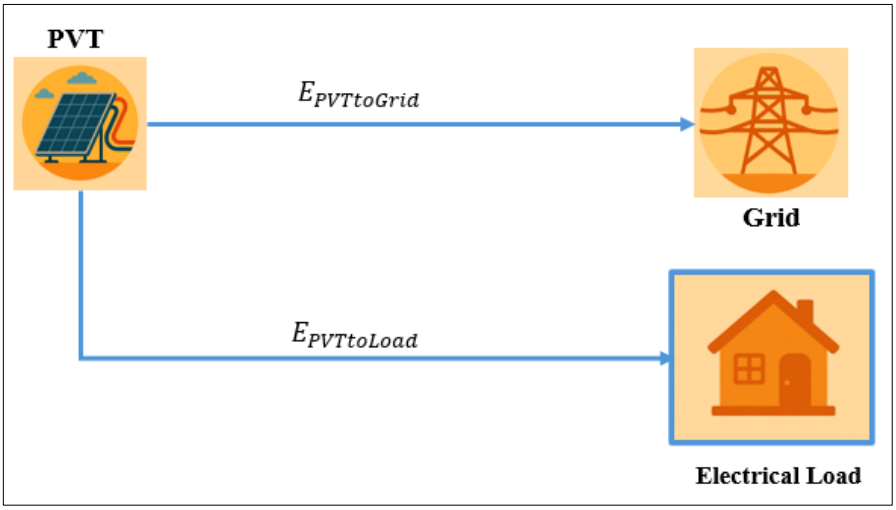

(c)

Figure 1. Energy Flow Diagram of the PVT-PCM Heat Pump System

3.1 Specification of the house and its heating and electricity load

The building characteristics and load profiles for İzmir, Türkiye were adopted from the literature (Bilir and Yıldırım 2018, 557). The examined house is a single storey detached house with a total floor area of 117 m² and consists of a living room, kitchen, bathroom and three bedrooms. Assuming that there are 4 people in the house, the housing settings defined in the Design Builder Software were used. The roof has a 30° tilt angle, and PV panels were considered to be installed on the south-facing side only. The indoor temperature was set as 20°C during the heating period, while the annual outdoor temperature for the specified location was taken hourly from the Meteonorm software. The heating load of the house was determined by considering the outdoor temperature and the general heat transfer coefficients of the building structural elements shown in Table 2, while the electrical load was considered to include the electricity demand for domestic hot water (DHW), lighting and household appliances and was determined using the Design Builder software.

Table 2. Overall heat transfer coefficient (U) for construction components (Bilir and Yildirim 2018, 557)

Components	**Values ($\mathbf{W/m^2K}$)**
Wall	0.7
Roof/Ceiling	0.45
Floor	0.7
Window	2.4

3.2 Climate and Radiation Data

The thermal and electricity output of PV/T depends on environmental variables such as temperature, solar radiation and wind speed. The formers were taken from Meteonorm via PVSOL software while the latter was retrieved from the PVGIS database during the period from January 2023 to December 2023, with an hourly resolution for Izmir. Figure 2 shows the monthly averages of ambient temperature, wind speed and global horizontal solar radiation over the related one-year period. Ambient temperatures reach their maximum in July and August, averaging around 30 °C, and drop to their lowest in January, at about 8 °C. Similarly, GHI values fluctuate throughout the year, peaking at

approximately 250 kWh/m² in July and falling to around 60 kWh/m² in December. Wind speeds remain relatively steady throughout the year, averaging between 2.5 and 3 m/s.

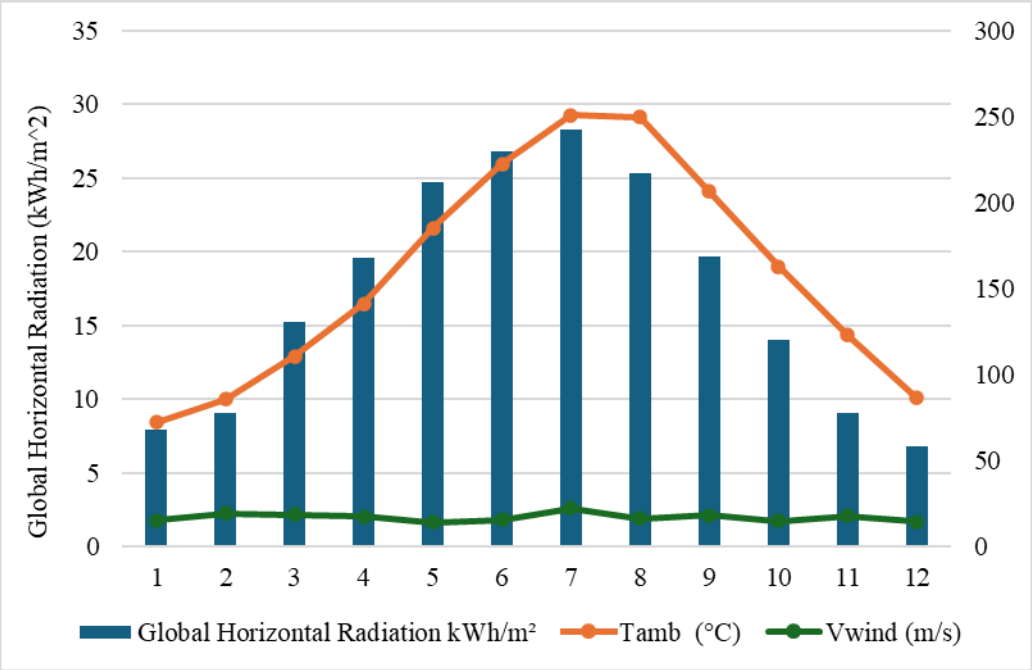

Figure 2. Monthly Distribution of GHI, T_{amb}, and V_{wind} in Izmir

3.3 Component Selection

3.3.1 Heat pump

In this study, the seasonal coefficient of performance (SCOP) value of the heat pump system was assumed to be 3.5 considering the warm climate of Izmir and reported SCOP values for Mediterranean regions (Mouzeviris and Papakostas 2022,14). This number aligns with EU Eco-design Directive (minimum SCOP≥3.1 for high temperature heat pump with 55°C water outlet) (European Commission 2013), which is accepted in Turkey as well. Based on the related constrains, a Samsung brand 5kw R32 Monobloc Air Source Heat Pump model with a common standard radiator system was selected as representative heat pump model, which has SCOP value of 3.5 for a flow temperature of 50°C.

To reflect this selection, the main technical specifications of the chosen Samsung 5 kW R32 Monobloc ASHP are summarized in Table 3. These parameters (including SCOP = 3.5 at 50 °C) are used in the model and subsequent techno-economic analysis.

Table 3. Technical Specifications of the Heat Pump

Feature	**Specification**
Model	Samsung 5 kW Monobloc ASHP
SCOP (@50°C, MCS database)	3.5
Heating Output	5kW
Refrigerant	R32 (Low GWP)

3.3.2 PV Panel

In this study, JAM72D30-550/MB monocrystalline silicon photovoltaic (PV) module was selected due to its high-power output. The electrical parameters used in the study are based on the manufacturer's data sheet and are given in Table 4.

Table 4. Technical Parameters of the Selected PV Module (JA Solar,2025)

Parameter	**Values**
PVT area	2.6 m^2
$\eta_{el,ref}$	0.213
Maximum Power	550 W
Temperature Coefficient	-0.35 %/°C
Reference Temperature	25 °C
Reference Global Radiation	1000 W/m^2

3.3.3 PCM materials

The selection of suitable PCMs for domestic heating applications mainly depends on their melting temperature and thermal properties. The melting-temperature range of

PCMs commonly used in residential heating systems typically lies between 20–32 °C (Tyagi and Buddhi 2007, 1151). The optimal melting point can change significantly depending on the integration method, location, the properties of the building (such as walls, floors, or dedicated storage units), and the type of PCM—organic, inorganic, or eutectic. Table 5 shows an overview of the properties and cost parameters of selected PCMs frequently cited in the literature.

Table 5. PCM properties

REF	Type of PCM	Latent heat (kJ/kg)	Melting Temperature (°C)	Density (kg/m^3)	Cost
Yao et al. (2020)	Na2HPO4·12H2O	265	32	1507	8.15$/kWh
Wijesuriya, Brandt, and Tabares-Velasco (2018)	Paraffin RT27	115	23	801	62.7 $/kWh
(Dimassi, Dahmouni, and Oueslati 2025)	Paraffin	250	26	950	29.5 $/kWh
(Pereira da Cunha and Eames 2016)	Calcium chloride hexahydrate	125	30	1710	2.71$/kWh
	Sodium sulphate decahydrate	**180**	**32**	**1485**	**1.35$/kWh**

Sodium sulfate decahydrate (Glauber's salt) was selected as the PCM in this study because it has a suitable melting point (~32°C) for residential heating applications and offers high latent heat capacity at the lowest cost. Sodium sulphate decahydrate, also known as Glauber's salt, is one of the recommended PCM materials for residential heating applications within the 32°C phase change temperature Hirschey et al. (2018, 2).

3.4 Scenario-Based System Configuration

Three main system configurations were considered to determine the effects of PVT integration and thermal storage on the system performance and cost-effectiveness of a heat pump-based heating system.

Scenario 1 (HP only): This configuration consists of a grid-powered heat pump. It does not include a storage system or a PVT.

Scenario 2 (HP + PVT): In this scenario, photovoltaic-thermal (PVT) collectors are integrated into the heat pump to reduce grid dependency. The number of PVT modules was varied from small-scale (1 to 5) to large-scale (5 to 25) to investigate the impact of solar energy contribution on system performance. This configuration does not include thermal energy storage.

Scenario 3 (HP + PVT + TES/PCM): This configuration includes a phase change material (PCM)-based thermal energy storage system in addition to the heat pump and PVT. It allows the storage of excess thermal energy generated by the PVT collectors and its subsequent use for home heating. The number of PVT modules again varied between 1 and 5 and 5 to 25, while the TES capacity was studied in the range of 50-450 kWh.

For Scenario 3, the selected capacity of PCM was determined based on the maximum cumulative heat deficiency calculated for each heating month. In other words, the difference between heat load and generation were calculated on an hourly basis for a specific month of the heating season (e.g., January, February, March, April, October, November and December) from the first day of the related month to the last day and the cumulative heat deficiency was determined within the time series of the related month (e.g., January from 1st Jan 01:00 to 31th January 24:00).

CHAPTER 4

MODELLING APPROACH

Energy systems including air-source heat pump, photovoltaic thermal collectors and thermal energy storage units were considered to meet heating and electricity load of a house located in Izmir, Turkey. The thermal and electrical outputs of PVT were first determined by a mathematical model developed in MATLAB based on the climate data presented in Section 3.2 and validated by the experimental results given in the literature. After the validation, scenarios with different HP, PVT and PCM combinations were evaluated in terms of their technoeconomic performance. The thermal output of the heat pump was simply determined by considering seasonal coefficient of performance of the selected heat pump. The economic performance of the proposed systems was assessed through key indicators including LCOE, LCOH, IRR, and payback period (PP). Assumptions used in modelling, and the mathematical foundations of the models are detailed in the following sections.

4.1 Assumptions and Limitations

- The study only concerns the heating load and electricity demand due to domestic hot water, lighting and home appliances. Cooling demand and other potential loads were not considered.
- Heat pump was considered to supply heat with a constant coefficient of performance throughout the heating period. The related constant COP was taken as the seasonal coefficient of performance of the heat pump from the manufacturer specification sheet for a common standard radiator system with a flow temperature of 50°C.
- Thermal storage unit was assumed to operate with 100% round trip efficiency, i.e., there is no energy loss during charging and discharging.
- Each cell in the PV modules was considered to have same temperature distribution and radiation intake.

- The effect of PV cell temperature on efficiency is assumed to be linear.
- It is also presumed that the optical and electrical losses of the panel are constant value and do not change over time.
- In particular, the effects of soiling, shading and aging are ignored. The optical losses of the panel are assumed to be constant, and effects such as pollution and shading are ignored.
- It is considered that the panel electrical output power changes linearly with radiation, and partial shading, spectral change and angle-dependent radiation losses are ignored.
- Even though the series and parallel resistance losses (diode losses, conductor losses etc.) within the cell are considered in advanced models, in this study, it is assumed that the module efficiency is constant, and these losses are indirectly reflected in efficiency.
- In this study, heat and electricity production are modeled with separate equations. Therefore, only the τα multiplier, which represents the part converted to heat, is used. The τα value is assumed to be 0.8.
- The slope of the surface was taken as β=45° in this study.
- Since the PVT system operates as an open-loop system, meaning it directly uses mains water, the inlet fluid temperature is assumed to be equal to the ambient temperature.
- In this study, the heat transfer coefficient of the fluid (h_f) is not calculated dynamically. Instead, since the structure of the system is like the systems in those studies, the constant value of h_f = 500W/m²K used in the literature was used here as well. This value is valid for water-based systems under similar flow rate and design conditions and is accepted as an assumption that will not significantly affect the accuracy of the model (Bahaidarah et al. 2013,448; Tiwari and Sodha 2006, 755).

$$\alpha\tau_{eff} = \tau_g * (\alpha_c * \beta_c + \alpha_T * (1 - \beta_c) - \eta_c * \beta_c \quad (1)$$

Table 6 summarizes the parameters used to verify the model's performance. For the validation step, several values were intentionally set differently from the final settings used in the scenario analyses so that the model outputs are directly comparable with those reported in the reference study.

Table 6. Assumptions and input parameters used in model validation

Quantity	**Symbol**	**Value**	**Unit**	**Source / Notes**
PVT aperture area	A_{PVT}	1.24	m^2	Bahaidarah et al. (2013)
Mass flow rate	$\dot{m}$	0.02	$kg \cdot s^{-1}$	Bahaidarah et al. (2013)
Collector efficiency factor	F'	0.828	-	Calculated from Bahaidarah et al. (2013)
Convective heat-transfer coeff.	h_f	500	$W \cdot m^{-2} \cdot K^{-1}$	Tiwari & Sodha (2006a)
Effective optical efficiency	$\alpha\tau_{eff}$	0.62	-	Computed with Eq. (1) using parameters from Bahaidarah et al. (2013),
Sky temperature relation	T_{sky}	Tamb-6	°C	Bahaidarah et al. (2013)

The assumptions made for the economic analysis are stated below:

- The Dollar Exchange Rate for April 2025 is 1TL=0.026$
- Interest rate was taken as 0.05 based on the data from Central Bank of the Republic of Turkey (CBRT, 2025)
- The electricity price for residentials was taken as 0.066$/kWh from Energy Market Regulatory Authority (EPDK)
- For residential applications, electricity sales to the grid are 0.011 $/kW EPDK (2025).
- The system life for PVT, heat pump and PCM was accepted as 25 years.
- O&M cost for PVT and HP was assumed to be 1% of installation costs.

4.2 Thermal Modelling of PVT

The study presents both numerical and experimental analyses of a PVT unit, indicating strong agreement between the theoretical and experimental results (Bahaidarah et al. 2013, 447). Given the reliability of the model, the same modelling approach outlined in this reference was used in the present study to develop the thermal model of the PVT system. The schematic representation of the PVT unit used in the model is shown in Figure 3.

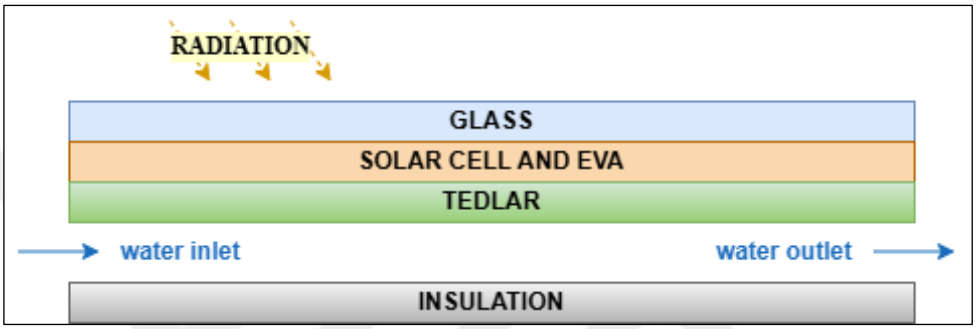

Figure 3. Layers of PVT (adapted from Bahaidarah et al. 2013, 447)

As shown from the Figure 3, the PVT unit consists of a single glass, solar cells, EVA, Tedlar, collectors and insulation, whose physical properties are listed in Table 6. Based on the multilayered configuration of the PVT unit, a one-dimensional thermal resistance diagram was developed. This enables a systematic analysis of conductive, convective, and radiative heat flows and forms the basis for the mathematical formulation presented in the following parts.

Table 7. Physical Parameters of Layers adapted from (Bahaidarah et al. 2013, 448).

Parameter	Value	Unit	Explanation
Lg	0.03	m	The thickness of glass cover
Kg	1	W/mK	The conductivity of glass cover
τ_g	0.95	-	The transmissivity of glass cover
ϵ_g	0.9	-	The emissivity of PV/Tair collector
α_c	0.85	-	The absorptivity of solar cell,
α_T	0.50	-	The absorptivity of tedlar
Lsi	$300*10^{-6}$	m	The thickness of silicon solar cell
Ksi	0.036	W/mK	The conductivity of silicon solar cell
Lt	0.0005	m	The thickness of Tedlar
Kt	0.033	m	The conductivity of Tedlar
Li	0.05	m	The thickness of back insulation,
Ki	0.035	W/mK	The conductivity of back insulation
s	0.05	m	The duct depth,
β_c	0.83	-	The packing factor of solar cell

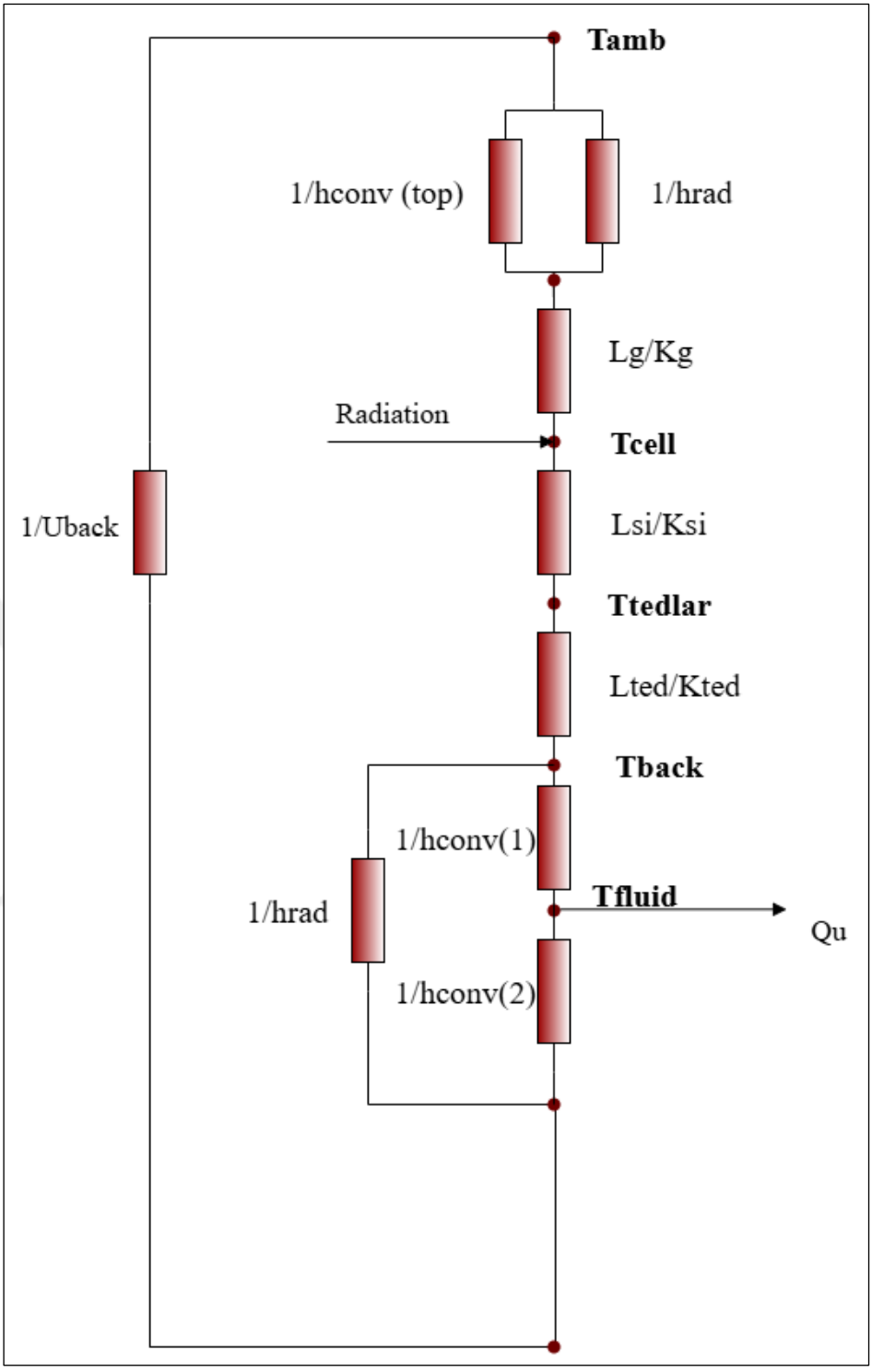

Figure 4.Thermal resistance circuit diagram for a PV/T water cooled system. in (adapted from Bahaidarah et al. 2013)

Based on the thermal resistance diagram, the useful thermal energy gain Q_u from the collectors was calculated using the following equation:

$$Q_u = Ac * FR * (hp1 * hp2 * \alpha\tau * G_T - (UL * (T_{f,in} - T_{amb}))) \quad (2)$$

where Ac is PVT area, $\alpha\tau$ the effective optical efficiency, T_{amb} is the ambient temperature, G_T is the radiation incident of the tilted PVT panel, which was determined as follows:

$$G_T = G_b R_b + G_d A_i R_b + G_d (1 - A_i) \left(\frac{1+cos\beta}{2}\right) + G\rho_g \left(\frac{1-cos\beta}{2}\right) \quad (3)$$

where G_b and G_d represent the beam and diffuse components of solar radiation incident on a horizontal surface, respectively, while G_T denotes the total solar radiation incident on the tilted surface. The parameter A_i known as the anisotropy index, is defined as the ratio of beam radiation to extraterrestrial radiation. The term R_b corresponds to the geometric factor, which quantifies the ratio of beam radiation received on a tilted surface to that on a horizontal plane. Additionally, β denotes the tilt angle of the photovoltaic (PV) module, representing the inclination of the panel relative to the horizontal surface. Lastly, ρ_g refers to the ground reflectivity, which is assumed to be 0.2 for residential areas. The geometric factor R_b was determined using the following equation:

$$R_b = \frac{cos\theta_z}{cos\theta} \quad (4)$$

Here, θ_z represents the zenith angle,

$$cos\theta_z = cos\,\phi cos\,\delta\,cos\,\omega + sin\,\phi\,sin\delta \quad (5)$$

θ denotes the angle of incidence. The incidence angle θ was determined using the following equation.

$$\theta = cos^{-1}[sin\,\delta\,sin\,\phi\,cos\,\beta - sin\,\delta\,cos\,\phi\,sin\,\beta\,cos\,\gamma + cos\,\delta\,cos\,\phi\,cos\,\beta\,cos\,\omega + cos\,\delta\,sin\,\phi\,sin\,\beta\,cos\,\gamma\,cos\,\omega + cos\,\delta\,sin\,\beta\,sin\,\gamma\,sin\,\omega] \quad (6)$$

ϕ is latitude (39.07º). δ is declination angle,

$$\delta = 23.45 \sin\left(360\ \frac{284+n}{365}\right) \quad (7)$$

n is the day of the year.

$sin\,\gamma$ is solar azimuth angle,

$$sin\,\gamma = \frac{cos\,\delta\,sin\,\beta\,sin\,\gamma\,sin\,\omega}{cosa_s} \quad (8)$$

as is the solar altitude angle,

$$sin\ a_s = cos\phi \cos\,\delta\,cos\,\omega + sin\,\phi sin\,\delta \quad (9)$$

ω is the hour angle,

$$sin\,\omega = (t_s - 12hour)x\ 15°/\text{hour} \quad (10)$$

t_s is the solar time(hour) where, solar time is hours of the day from 1 to 24.

After the calculation of G_T, the other parameters required to determine the useful heat gain (Eqn 1) were determined as follows:

FR is the heat removal factor, which represents the efficiency of heat transfer from the absorber surface to the working fluid in the collector,

$$FR = \frac{\dot{m}*cp}{A_{c*}U_L} * \left(1 - \left(\exp\left(\frac{-A_{c*}U_{L*}F'}{\dot{m}*cp}\right)\right)\right) \quad (11)$$

$\dot{m}$ is the water mass flow rate, cp the specific heat capacity of water, F' is the collector efficiency factor. U_L is the total heat loses coefficient calculated with,

$$U_L = U_{tf} + U_b \quad (12)$$

U_{tf} is the overall heat transfer coefficient from glass to air through the cell and tedlar,

$$U_{tf} = \frac{U_{tT}*h_f}{U_{tT}+h_f} \quad (13)$$

The overall heat transfer coefficient from glass to tedlar through the cell U_{tT} calculated as follows,

$$U_{tT} = \frac{U_T \, x \, U_t}{U_t + U_T} \tag{14}$$

U_T the conductive resistance from the cell to flowing water through tedlar that can calculate with this formula,

$$U_T = \frac{1}{\frac{L_{si}}{K_{si}} + \frac{L_T}{K_T}} \tag{15}$$

L_{si} is the thickness of back insulation, K_{si} is the conductivity of silicon solar cell. The overall heat transfer coefficient from solar cell to ambient through glass cover U_t is calculated as follows,

$$U_t = \frac{1}{\frac{L_g}{K_g} + \frac{1}{h_{conv}} + \frac{1}{h_{rad}}} \tag{16}$$

L_g is the thickness of glass cover, K_g is the conductivity of glass cover, h_{conv} the convective heat transfer coefficient on the upper surface of the PVT module due to wind effect was calculated with the following formula

$$h_{conv} = 2.8 + 3 * V_{wind} \tag{17}$$

h_{rad} is the radiative heat transfer between the PV surface and the sky expressed in Equation 10.

$$h_{rad} = \epsilon_g \times \sigma \times ({T_{cell}}^2 + {T_{sky}}^2) \times (T_{cell} + T_{sky}) \tag{18}$$

where T_{sky} is the sky temperature and is taken as (Soytürk, Kizilkan, And Ezan 2022,148).

$$T_{sky} = 0.0552 * {T_{amb}}^{1.5} \tag{19}$$

σ is Stephen-Boltzmann constant, T_{cell} is temperature of cell:

$$T_{cell} = ((\alpha\tau * G + U_t * T_{amb} + U_T * T_{bs}) / (U_t + U_T)) \tag{20}$$

T_{bs} is the back surface temperature,

$$T_{bs} = (h_{p1} * \alpha\tau * G + U_{tT} * T_{amb} + h_f * T_f) / (U_{tT} + h_f) \quad (21)$$

where h_f is heat transfer coefficient of fluid, T_f is the fluid mean temperature,

$$T_f = \frac{(T_{fout}+T_{fin})}{2} \quad (22)$$

where T_{fin} representing the fluid inlet temperature, is assumed to be equal to the ambient temperature. T_{fout} fluid outlet temperature,

$$Tf_{out} = T_{amb}\left(\frac{h_{p1}*h_{p2}*\alpha\tau*G}{U_L}\right)*\left(1\left(\frac{1-\left(\exp\left(\frac{-A_{c*}U_{L*}F'}{\dot{m}*cp}\right)\right)}{\frac{A_{c*}U_L}{\dot{m}*cp}}\right)\right)+Tf_{in}\left(\frac{1-\left(\exp\left(\frac{-A_{c*}U_{L*}F'}{\dot{m}*cp}\right)\right)}{\frac{A_{c*}U_L}{\dot{m}*cp}}\right) \quad (23)$$

$hp1$ is the penalty factor due to the tedlar through the glass,

$$h_{p1} = \frac{U_T}{U_t + U_T} \quad (24)$$

is the penalty factor due to interface between the tedlar and working fluid,

$$h_{p2} = \frac{h_f}{(U_{tT} + h_f)} \quad (25)$$

U_b is an overall heat transfer coefficient from bottom to ambient,

$$U_b = \frac{1}{\frac{L_i}{K_i}+\frac{1}{h_{conv}}} \quad (26)$$

4.2.1 Electrical Modelling of PVT

The electrical output of the PVT unit was calculated as follows:

$$P_{el} = \eta_{el} * A_c * G_T \quad (27)$$

where η_{el} is electrical efficiency of PVT and calculated as:

$$\eta_{el} = \eta_{ref} * (1 - \beta * (T_{cell} - T_{amb})) \quad (28)$$

4.3 Heat pumps

The electrical energy required for the heat pump was determined by considering the heat load and seasonal coefficient of performance taken for this study (see section 3.3.1) as follows:

$$\mathbf{SCOP} = \frac{\mathbf{Q_{heatingload}}}{\mathbf{W_{comp}}} \quad (29)$$

where $Q_{heatingload}$ is the seasonal space-heating demand (kWh) and W_{comp} is the compressor electricity (kWh). SCOP value was assumed to be the constant (3.5) for all heating periods.

4.4 Thermal Energy Storage

The amount of thermal energy stored in the PCM (Q_{PCM}) was calculated by the following equation:

$$Q_{PCM} = m_{PCM} * H_{PCM} \quad (30)$$

where, m_{PCM} is weight of PCM (kg), H_{PCM} is latent heat (kJ/kg).

4.5 Economic Analysis

The economic performance of the proposed systems was investigated for different scenarios. The lifetime of the considered system was taken as 25 years and Net Present Value (NPV) and Levelized Cost of Heat (LCOH), Levelized Cost of Energy (LCOE), Internal Rate of Return (IRR) and Payback Period (PP) were used as economic performance indicators. They were used to compare the return on investment and cost-effectiveness of the systems under study.

Internal Rate of Return (IRR): It is the discount rate that equates the present value of an investment's expected cash flows to zero and indicates the annual rate of return on the investment.

$$\boldsymbol{IRR} \longrightarrow NPV = \sum_{t=1}^{N} \frac{CF_t}{(1+IRR)^t} - C_{cap} = 0 \tag{31}$$

where t represents year, C_{cap} is total initial investment cost of the system, CF_t is the net annual cash flow, which consists of electricity savings, gas savings, and export revenues, minus the fixed operation and maintenance (O&M) costs. at the end of the period N, N is the service life of the project. The initial investment cost, operation and maintenance costs are shown in Table 8. The base interest rate and system lifetime were taken as 5% and 25 years.

Levelized Cost of Heat (LCOH): It is an economic indicator used for heating systems. It calculates the average cost of producing thermal energy per unit over the system's lifetime. Following the approach presented in the literature, the Levelized Cost of Heat (LCOH) is calculated as follows (Yang et al. 2021, 3):

$$LCOH = \frac{C_{cap,heating} + \sum_{t=1}^{n} \frac{O\&M_t + (\sum E_{HP} * p_{buy})}{(1+r)^t}}{\sum_{t=1}^{n} \frac{Q_{heating\ load}}{(1+r)^t}} \tag{32}$$

where $C_{cap,heating}$ is the capital cost for heating system, n is the system lifetime,$O\&M_t$ is the operational and maintenance cost in year t, $E_{HP} * p_{buy}$ is the total annual cost of grid electricity consumed by the heat pump and r is the discount rate, $Q_{heating\ load}$ is the annual heating load of house.

Levelized Cost of Electricity (LCOE): The Levelized Cost of Electricity (LCOE) is a widely used economic indicator that expresses the average cost of producing electricity over the lifetime of an energy system, discounted to present value.

$$LCOE_{el} = \frac{C_{PVT} + \sum_{t=1}^{n} \frac{O\&M_t + \left(\left(\sum E_{grid\ to\ load} - \sum E_{HP}\right) * p_{buy}\right) - \sum E_{PVTtogrid} * p_{sell}}{(1+r)^t}}{\sum_{t=1}^{n} \frac{E_{el,load}}{(1+r)^t}} \tag{33}$$

C_{PVT} is the capital cost of PVT system, $\sum E_{grid\ to\ load}$ is total electricity purchased from the grid to cover the building's electrical demand (including the HP). $\sum E_{PVTtogrid}$ is the electricity generated by the PVT system and exported to the grid. $E_{el,load}$ is the annual building electricity demand excluding the HP consumption (lighting, appliances, etc.).

$$LCOE_{TOTAL} = \frac{C_{cap,el} + \sum_{t=1}^{n} \frac{O\&M_t + \left(\left(\sum E_{grid\ to\ load}\right) * p_{buy}\right) - \sum E_{PVTtogrid} * p_{sell}}{(1+r)^t}}{\sum_{t=1}^{n} \frac{E_{el,load} + \left(\frac{Q_{heatingload}}{SCOP}\right)}{(1+r)^t}} \quad (34)$$

$C_{cap,el}$ is the capital cost for the energy system, C_{el} is cost of grid electricity, $E_{el,load}$ is the total electricity load of the house.

To calculate IRR, LCOH, $LCOE_{el}$ and $LCOE_{TOTAL}$ values, the prices of components and operational costs shown in Table 8 were used.

Table 8. Component, Energy and Maintenance Costs

Parameter	**Price**	**Unit**	**Ref**
Electricity price for residentials (p_{buy})	0.066	\$/kWh	EPDK(2025)
Electricity sales price to the grid (p_{sell})	0.011	\$/kWh	EPDK(2025)
PVT	200	$\$/m^2$	(Shboul et al. 2024,144)
Inverter	180	\$/kW	(Shboul et al. 2024,144)
Heat Pump (5kW)	2148	\$	(The Heat Pump Warehouse 2025)
O&M cost	%1 of capital cost	\$	(Shboul et al. 2024,144)
PCM material cost	1.35	\$/kWh	(Pereira da Cunha and Eames 2016,230)
PCM storage tank	399.16	$\$/m^3$	(Plytaria et al. 2018)
Natural Gas	0.032	\$/kWh	(BOTAŞ, 2025)

Table 8 summarizes the baseline component costs and electricity tariffs used in the model. These entries serve as inputs to all IRR, $LCOH$, $LCOE_{TOTAL}$ and $LCOE_{el}$ calculations and are varied in the sensitivity analyses.

This study did not include a comprehensive structural design of the PCM tank. Instead, for the purpose of comparative energy and economic analysis, a representative tank cost was taken from the available literature. According to reference study, the cost of a PCM tank was estimated at €350/m³ ($399.16/m³ in USD) (Plytaria et al. 2018, 633). Installation and auxiliary system costs were ignored in this analysis.

4.6 Energy Management Strategy

For the technoeconomic analysis of the considered scenarios, energy management algorithms were developed to ensure the heating and electricity load of the selected house are fully covered by heat pump, PVT, thermal storage unit and grid combinations (see Figure 1). A time series simulation was performed for one calendar year with hourly time steps to determine dynamic behavior of systems. Starting from January 1 for each hour, the required heat and electricity loads were determined and the heat and electricity generation by PVT were calculated. If the heat generated by PVT is greater than the heat load, the excess heat is used to charge PCM materials till its maximum capacity. For the cases where PCM reaches its maximum capacity, the surplus heat is dumped. On the other hand, if the heat by PVT is less than the heat load, the deficiency is first covered by PCM till its zero and then by the heat pump. For the electricity balance, if the electricity generated by the PVT exceeds the electrical load, the excess electricity is used for the heat pump's electricity needs or for the home's electrical needs, such as lighting and appliances. If the home doesn't need electricity, the excess electricity is sent to the grid. For the opposite case, the electricity deficiency is covered by the grid. The simulation ends when all hours in a year are covered and it gives the total heat provided by PVT, PCM and heat pump, the total electricity supplied by PVT and grid and the excess electricity sold to the grid annually. Thermal and electricity load coverages of each component and the corresponding LCOH, LCOE, and IRR values were calculated accordingly.

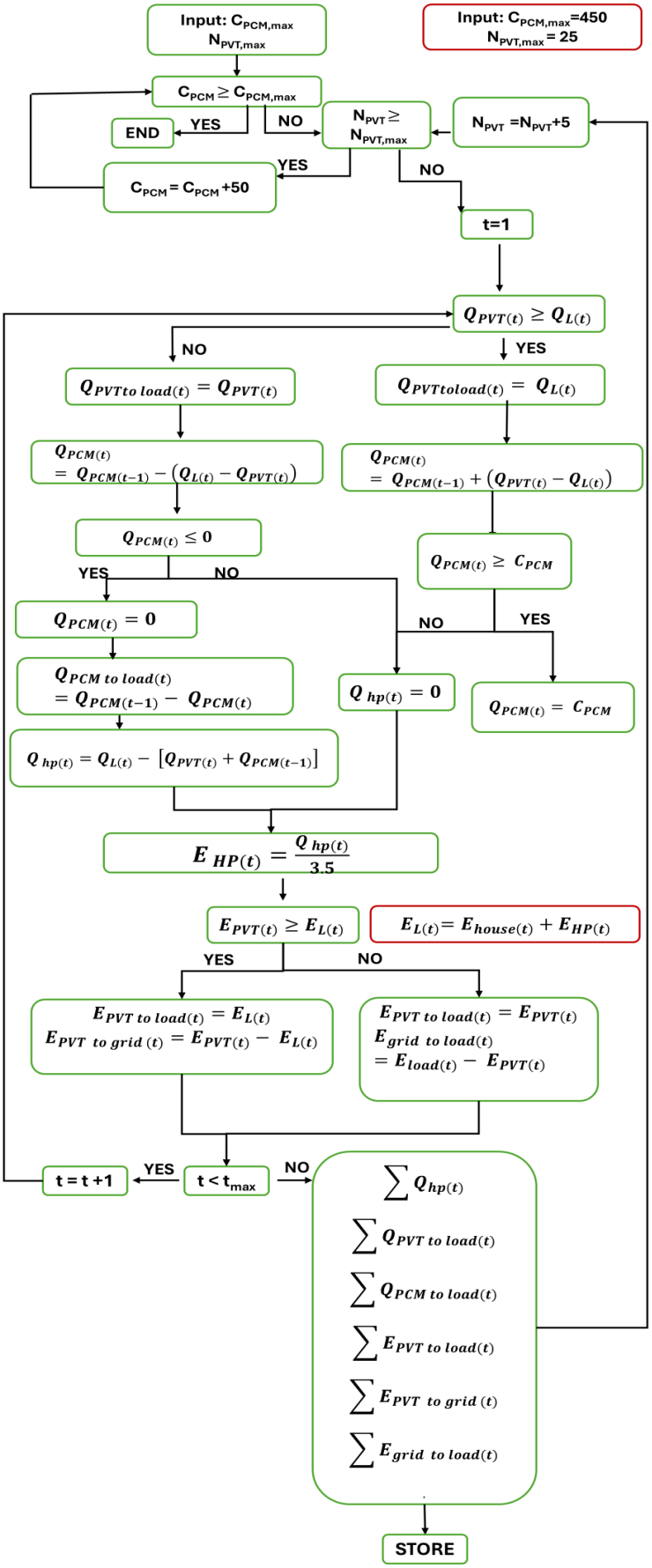

Figure 5. Flow Chart of Simulation Methodology

CHAPTER 5

RESULTS AND DISCUSSION

5.1 Validation of PVT Thermal model

The performance of the developed PVT model was validated against the results reported which include both experimental measurements and numerical simulations (Bahaidarah et al. 2013, 451). As a first step, the cell temperature of the PVT collector was determined under the same operating conditions described in the reference study. Figure 6 shows a comparison between the present model and the reference data.

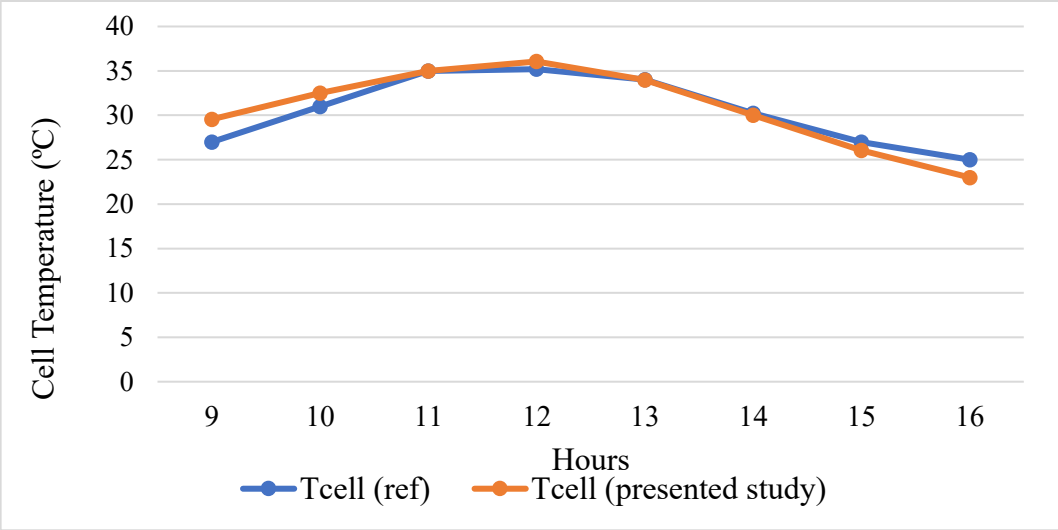

Figure 6. Comparison of Tcell values

The results indicate that the Mean Absolute Percentage Error (MAPE) is 3.63% and a maximum relative error of 9.37% was observed in the predicted cell temperature between our model and experimental results in the reference study. Considering standard practice in engineering analyses, errors below 10% are often deemed acceptable (Lewis 1982, 40).

The model is considered to reliably captures the thermal behavior of the PVT system. Therefore, it is suitable for further scenario-based performance and economic assessments.

After the validation of cell temperature, the consistency of model was further verified by comparing the predicted useful thermal energy and electrical power output of the PVT system with the corresponding results from (Bahaidarah et al. 2013, 8).

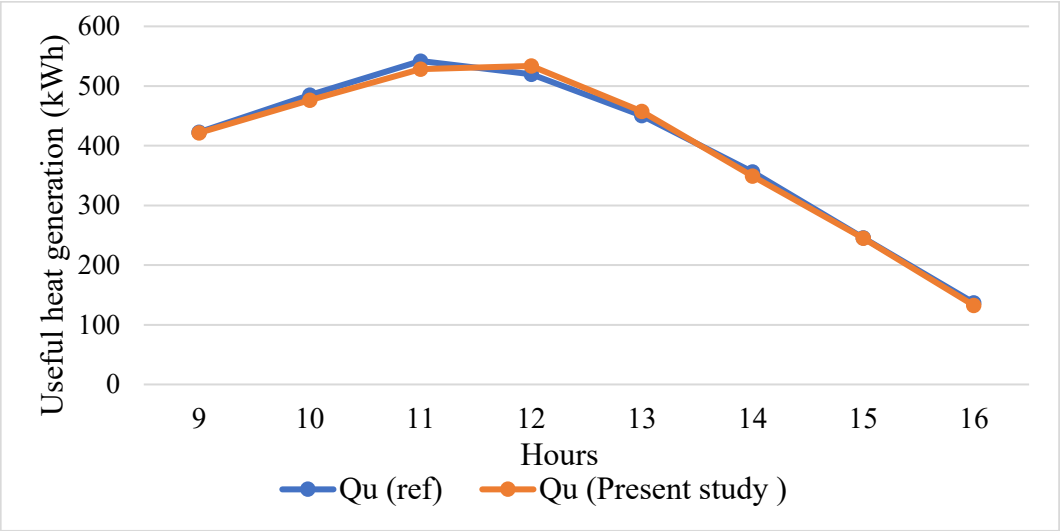

Figure 7. Comparison of Qu values

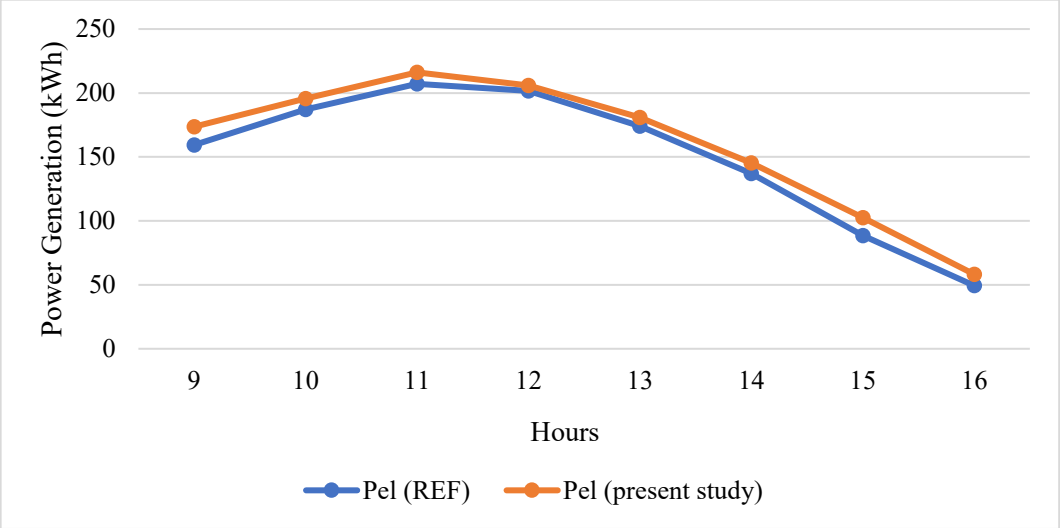

Figure 8. Comparison of Power Generation values

Figures 7 and 8 indicate these comparisons for heat and power generation, respectively. The results exhibit a good agreement was observed between the results in our model and in the reference study, with maximum relative errors of 3.21% for useful

heat and 7.65% for electrical power output. These outcomes further support the model's capability to reliably simulate both the thermal and electrical behaviour of the PVT unit under similar operating conditions.

5.2 Electrical and Thermal Output of the PVT System

After model validation, the useful heat and electrical power output of a single PVT unit were determined for PVT parameters specified in Section 4.2 by using climate data of İzmir, where the house is located. The monthly thermal and electrical power output of the PVT unit are shown for each month in Figure 9. According to the results, the annual thermal and electrical energy production of a single PVT collector is calculated as 2954.64 and 804.85 kWh, respectively. The area of the selected PVT unit is 2.6 m^2 and the corresponding area specific values are 1136.4 and 309.6 kWh/m^2, respectively. These numbers align with values reported in the literature; for example, annual heat and electricity generation of 1204.9 and 258.6 kWh/m² were found for a similar PV/T configuration and climate (Başaran and Koç 2024, 368).The relatively higher electricity generation observed in the related study compared to ours is ascribed to the additional cooling and higher efficiency of PV unit used in their study. The consistency of our results with the literature was also seen in daily basis analysis. On a representative day, thermal and electrical yields of 0.52 and 0.12 kWh/m² were reported for the system (Aste, Leonforte and Del Pero 2015, 94). On the same day under similar conditions, our model yielded 0.48 and 0.13 kWh/m^2. The consistency of our results with the literature was also seen in daily basis analysis. On a representative day, the study of (Aste, Leonforte, and Del Pero 2015) using a glazed PVT collector with an a-Si/µc-Si thin-film PV layer bonded to a roll-bond flat plate absorber, 50 mm rear mineral fiber insulation, and a mass flow rate of 0.066 kg/s, reported thermal and electrical outputs of 0.52 and 0.12 kWh/m^2. Under the same irradiance levels and at matching hours, our model yielded 0.48 and 0.13 kWh/m^2 The small differences can be attributed to different PV technology, absorber structure, insulation quality, and a lower mass flow rate in our system, affecting thermal heat removal and electrical performance.

The monthly thermal and electricity generation profiles were also analyzed and compared with the corresponding loads. Figure 9 shows that both thermal and electrical outputs increase during summer months and decrease in winter months as expected due to the corresponding changes in solar radiation in the related months.

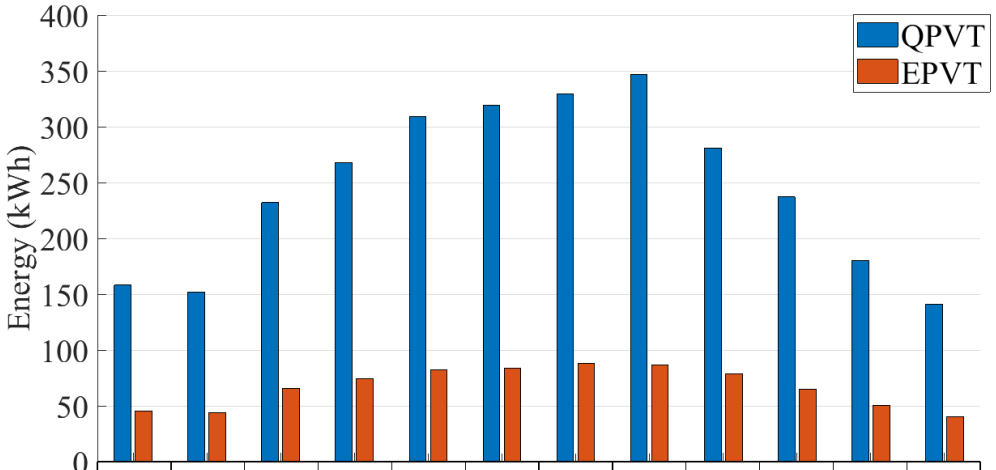

	Jan	Feb	Mar	Apr	May	Jun	Jul	Aug	Sep	Oct	Nov	Dec
QPVT	158	152	232	268	309	319	329	347	281	237	180	141
EPVT	45.5	43.8	65.6	74.3	82.6	83.7	88.4	86.7	78.8	64.8	50.3	40.3

Figure 9. Monthly PVT Energy Production

The maximum thermal and electrical outputs were calculated as 347 kWh and 88.4 kWh while the minimum values for the same parameters were found to be 141 and 40.3 kWh, respectively. The monthly profile of thermal and electricity generation of the PVT unit do not align the thermal and electricity demand patterns of the selected house (see Figure 10 and related explanation in Appendix A). While the heating load is mostly concentrated in the winter months and drops to zero during the summer, the electrical load almost remains constant throughout the year, resulting in a mismatch between energy supply and demand. The related mismatch is more pronounced for thermal energy supply and demand compared to electricity counterparts, indicating the importance of thermal energy storage for balancing demand and supply for the long term. The similar mismatch was also observed for the short term. Figure 10 shows the hourly thermal and electrical output of the photovoltaic-thermal (PVT) unit with the building heating demand on a representative winter day, January 15. The graph shows the periodic mismatch between the thermal output of the PVT unit and the thermal load of the house. The heating demand peaks in the early morning (06:00-09:00) and in the evening (20:00-23:00), when solar

radiation is at its minimum, which prevents the PVT system from producing sufficient energy, and the PVT systems cannot produce energy at night. This graph highlights the difficulty of aligning the thermal output of the PVT system with the demand. This further emphasized that the integration of thermal energy storage (TES) system to PVT units are essential to prevent imbalance between load and demand for both short and long term.

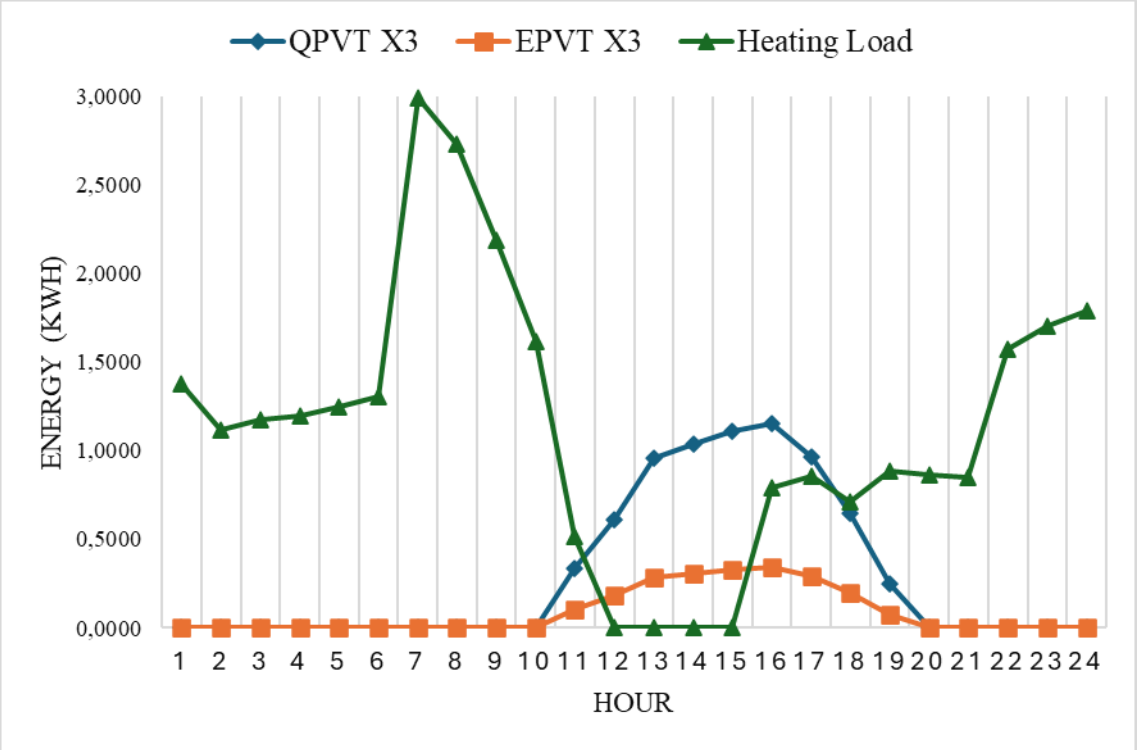

Figure 10. Hourly Energy Generation and Heating Demand on a Representative Winter Day (January 15)

For technoeconomic analysis, selecting an appropriate number of PVT unit is important to balance thermal performance, investment cost, and spatial limitations. In this study, a range of PVT numbers was considered to assess system behaviour and economic performance for different PVT integration. The upper limit was determined based on the constraint of the available south-facing roof area (72 m²), which can accommodate a 50 maximum of 25 collectors with a surface area of 2.6 m² for each. To evaluate system performance till this upper limit, the investigation considers a small-scale integration from 1 to 5 units, with an increment of 1, and a large-scale integration from 5 to 25 units, with an increment of 5.

5.3 Technoeconomic Assessment

Technoeconomic analysis of systems were performed for scenarios explained in Section 3.4. For each scenario, thermal and electricity energy output, electricity consumption, electricity sold to the grid and received from the grid, and heat and electricity load coverage rates were analyzed separately. and the economic performances of systems were evaluated for a 25-year system lifetime and a 5% discount rate by the selected performance indicators such as $LCOH$, $LCOE_{el}$, $LCOE_{total}$, and IRR. At the end of section all scenarios were compared in terms their technoeconomic performances and the effect of PCM capacity on the performance of the optimum HP-PVT-PCM combination was analyzed.

5.3.1 Scenario 1 (Only Heat Pump)

In Scenario 1, the annual heat load of 3037 kWh is fully covered with a heat pump powered by the grid while the annual electricity load of 2196 kWh is met by the grid; these load values are taken from Levent Yıldırım's study (Bilir and Yıldırım 2018, 562). Since the SCOP value of the heat pump was taken 3.5, the heat pump-related electricity consumption is 867.7 kWh. Considering the grid electricity price for household in Turkey and costs listed in Table 9, $LCOH$, $LCOE_{el}$, $LCOE_{total}$, and IRR values were calculated.

Table 9. Economical Parameters for Scenario 1 (Only Heat Pump)

Scenario	$LCOH$(\$/kWh)	$LCOE_{el}$ (\$/kWh)	$LCOE_{total}$ (\$/kWh)	IRR
Only Heat Pump	0.0761	0.066	0.123	-0.048

As seen from Table 9, the negative IRR value shows that the investment is not recoverable within the system lifetime. The LCOH of the only heat pump scenario (0.0761 \$/kWh) is more than twice the current natural gas price in Turkey (0.032 $/kWh).

5.3.2 Heating by the combined PVT and Heat Pump System without thermal storage (Scenario 2)

In Scenario 2, the PVT system and heat pump work together to meet the house's thermal load. The heat generated by the PVT is transferred directly to the building load, while the unmet thermal demand is met by the heat pump (see Figure 1). The electricity generated by the PVT is used to meet the electricity load when it is sufficient and in case of overproduction its surplus is sent to the grid. On the other hand, when the PVT's output is insufficient, the grid covers the electrical load.

The operating characteristics of the integrated PVT and heat pump system in Scenario 2 were assessed by analyzing the annual contribution of each component to the heating and electricity loads. The PVT's and heat pump's contribution to the heating load, alongside the PVT's and grid's shares of the electricity load, are shown in Figure 11. As seen from Figure 11a, the PVT contribution to the heat load increases only slightly with system size and its share remains below 20% even for 25 PVT indicating that the heat pump is the primary heat source. This is due to the mismatch between demand and generation, as previously illustrated in Figure 10. For electricity load, PVT exhibits a higher coverage ratio reaching almost 40% for maximum PVT number, which is attributed to a relatively lower mismatch between electricity demand and generation.

Figure 11 shows, in simple terms, how adding more PVT modules changes who carries the load. Panel (a) splits the heating between the PVT and the heat pump, while panel (b) shows how the electricity need is shared between PVT generation and the grid.

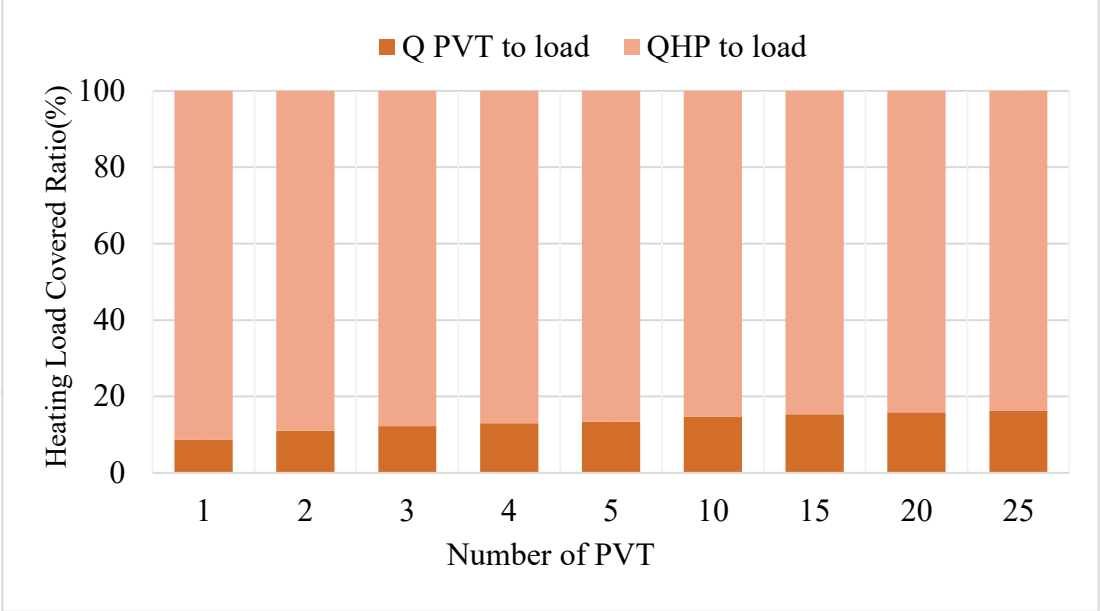

(a)

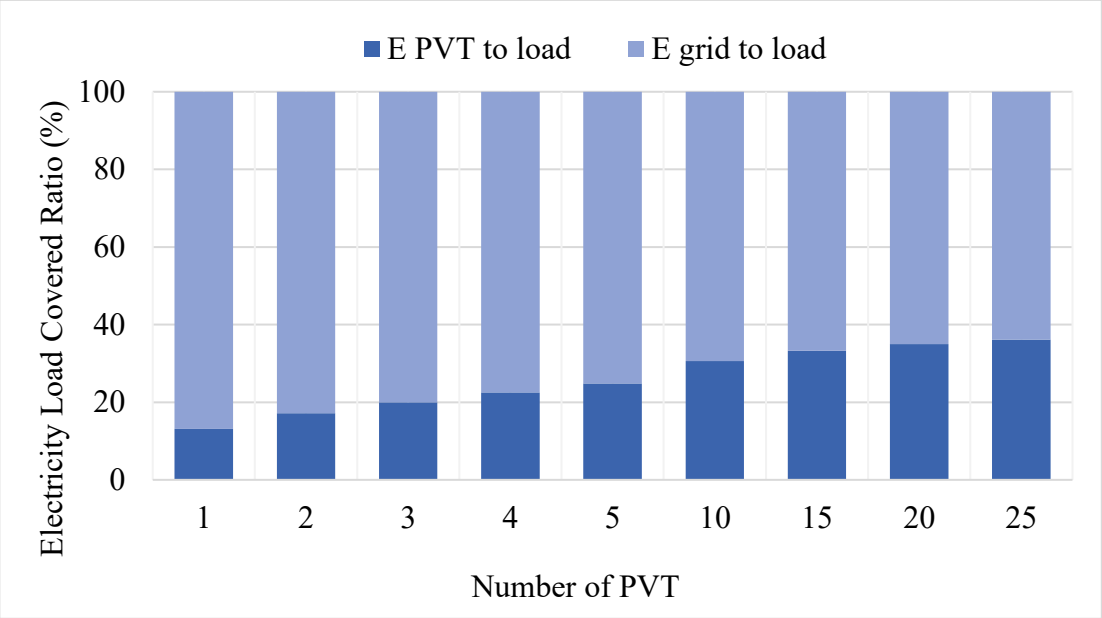

(b)

Figure 11.Heating (a) and Electricity (b) Load Coverage Ratios for Scenario 2

As seen in Figure 11 (a), the PVT's ability to meet the heat load increases slightly with the number of modules, with the heat pump providing most of the heat load. This is

due to the mismatch between demand and generation, as previously illustrated in Figure 10. In Figure (b), the electricity share provided by the PVT system increases significantly as the number of modules increases, leading to a decrease in grid dependency. Overall, the heat pump maintains its dominance on the thermal side, while the PVT system has a stronger impact on the electrical load.

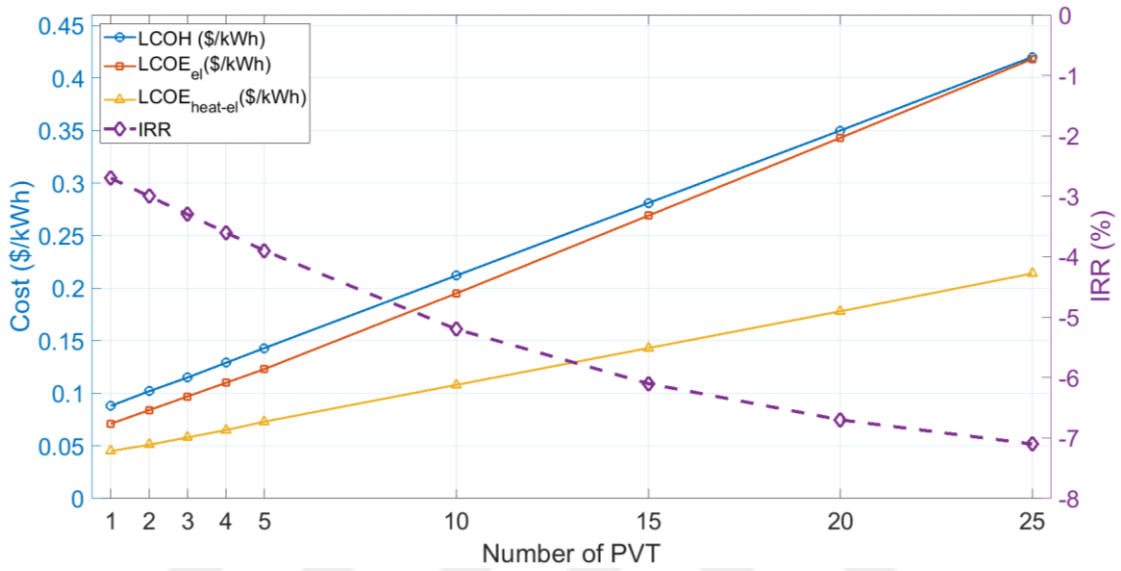

Figure 12. Economic Performance Indicators of Scenario 2 for Different PVT Module Configurations

For technoeconomic assessment, the effect of PVT number on the economic performance indicators was also analyzed. As seen from Figure 12, Levelized costs increase with PVT capacity, demonstrating that overall system cost outweighs the savings due to the reduction in grid purchases. Among these indicators, $LCOE_{total}$ shows a more limited increase compared to the others thanks to the cumulative saving in both heat and electricity-based grid cost. Like levelized costs, the Internal Rate of Return (IRR) is also negatively affected by the number of PVT units. It shows a decreasing trend and remains negative across the considered capacity range. The results suggest the enhanced energy coverage achieved with a higher PVT number does not translate into economic feasibility under the present conditions. This is mainly related to the strong mismatch between load and generation and the resulting low coverage ratios for both heat and electricity load, which signifies the importance the energy storage. This will be evaluated in the following sections.

5.4 Heating by the combined PVT and HP system with Thermal Storage (Scenario 3)

In Scenario 3, the heating demand is covered by the combined operation of the PVT system, the heat pump, and the thermal storage unit, as illustrated in Figure 1a. The PVT collector provides useful heat directly to the load or stores it in PCM, while the heat pump supplies the remaining demand. On the electrical side, the PVT system contributes to the building's electricity needs and can also feed excess power to the grid, with any deficit supplied from the grid (Figure 1b–c).

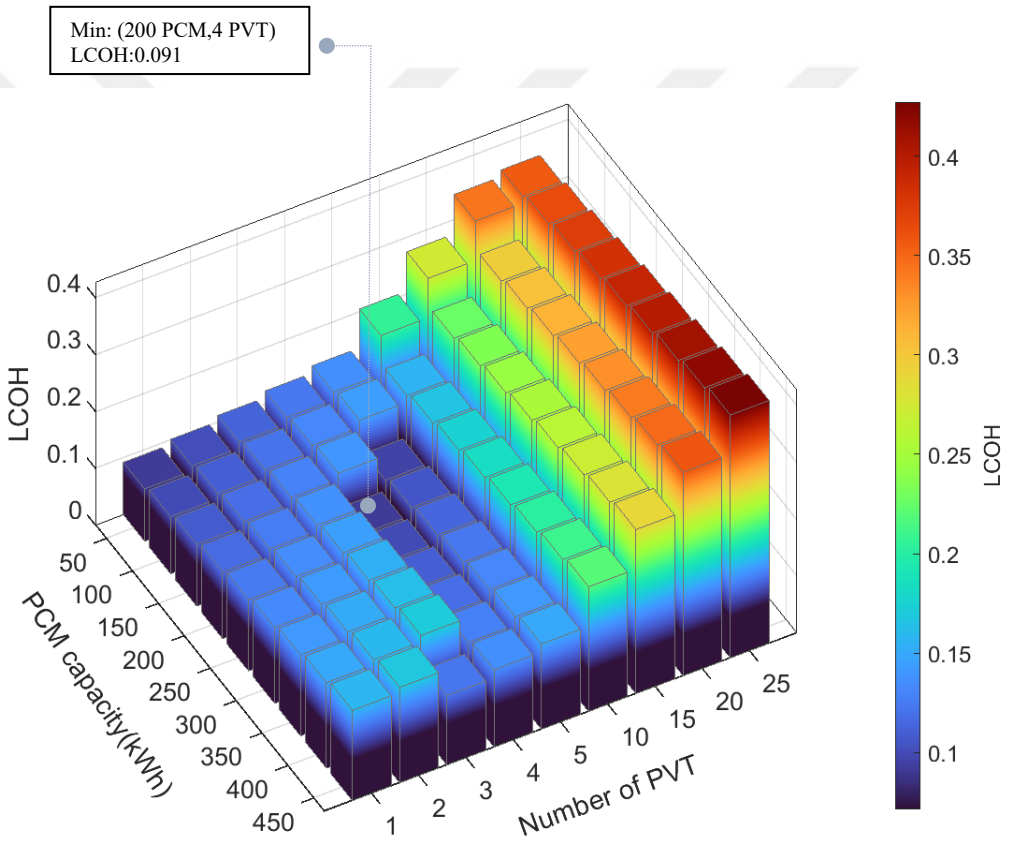

Figure 13. $LCOH$ Variation with PCM Capacity and PVT Modules

For Scenario 3, the technoeconomic performance of the systems were first evaluated for various PVT numbers (1-25) and PCM capacity (50-450 kWh) and the best case was determined based on the considered economic performance indicators. Then the operating characteristic of the selected configuration was analyzed. Figure 13 shows the variation of the $LCOH$ value with the number of PVT modules and the PCM capacity. As seen from the figure, although the $LCOH$ value initially appears lower at low PCM

capacity (e.g., 50 kWh), the heat pump runs more often because the storage cannot adequately cover the heat load, which increases the electricity purchased from the grid and raises the $LCOH$. Conversely, increasing the number of PVT modules raises the capital cost, but the reduction in grid dependence due to the additional heat generation has a downward effect on the $LCOH$. This effect is particularly significant in medium sized configurations; for instance, a 200 kWh PCM and four PVT modules achieve a minimum $LCOH$ of \$0.091/kWh (see Appendix C for detailed numerical values). At high PVT capacity (e.g. 25 PVT modules), the increase in system cost becomes dominant, with $LCOH$ reaching approximately \$0.42/kWh. These results indicate that the optimal configuration is achieved with moderate PCM capacity and a limited number of PVT modules.

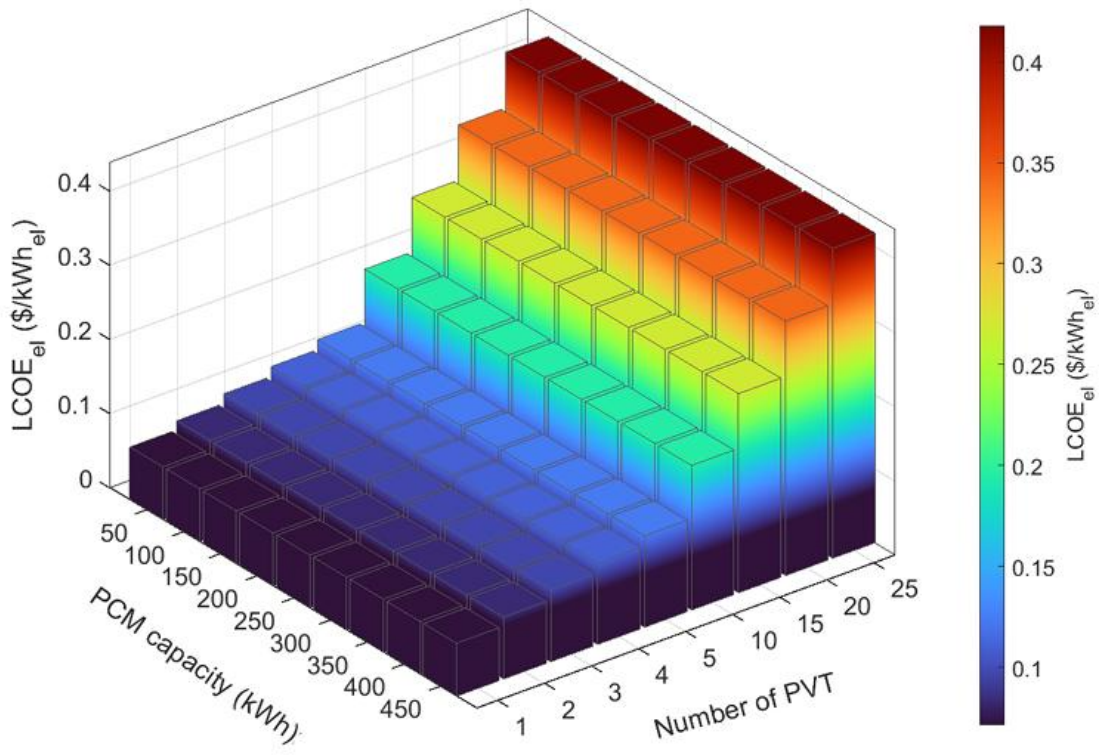

Figure 14. Variation of $LCOE_{el}$ with the Number of PVT Modules

Figure 14 shows how the levelized cost of electricity from the PVT system $LCOE_{el}$ changes with the number of PVT modules. In this figure, $LCOE_{el}$ is defined as the discounted capital and O&M costs on the PVT-electricity side divided by the PVT kilowatt-hours that are self-consumed by household electrical loads (lighting and

appliances); heat production, the heat pump, and PCM are outside this metric. The curve increases as the number of modules grows because investment rises while self-consumable electricity is limited by the load profile, so a larger share of the extra generation is exported to the grid. Since the feed-in price is lower than the purchase price ($psell < pbuy$), export revenue does not fully offset the added cost. As a result, the lowest $LCOE_{el}$ occurs with small PVT systems, and the cost metric rises at larger sizes as the self-consumption ratio declines.

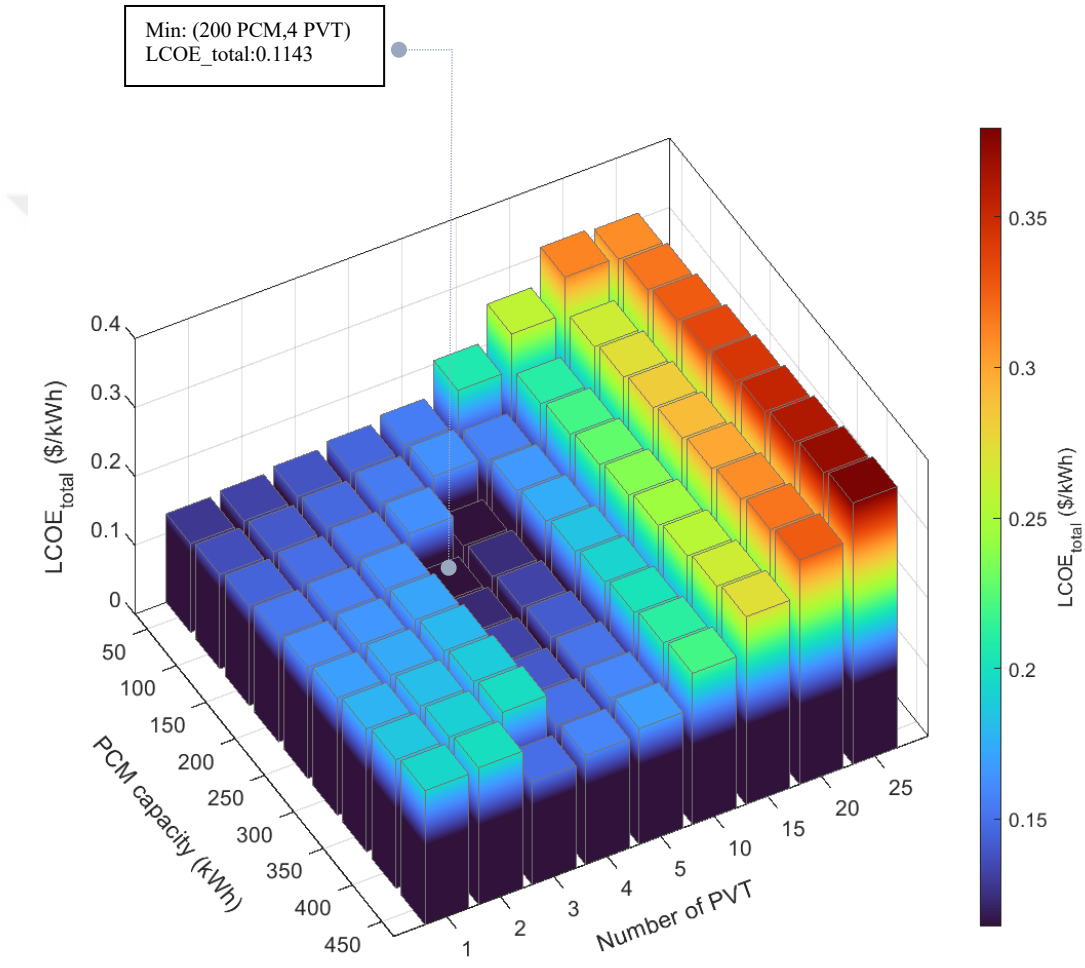

Figure 15. Variation of $LCOE_{total}$ with PCM Capacity and Number of PVT Modules

The effect PVT number and PCM capacity on the system economic performance was also evaluated by using $LCOE_{total}$, which considers both heat and electricity load coverage. Figure 15 presents $LCOE_{total}$ as a function of the number of PVT modules and PCM capacity. Consistent with Figure 13 (LCOH), the surface reflects a clear trade-off: with low PCM, storage is insufficient, the heat pump operates longer, and grid purchases increase; as PCM capacity grows, this dependence declines. By contrast, at very high

PVT units (about 20–25), capital cost becomes dominant and $LCOE_{total}$ rises above \$0.35/kWh. The lowest values occur with moderate storage (approximately 200–250 kWh) and a modest collector field (about 3–5 modules). In line with this pattern, the HP only case in Table 8 yields $LCOE_{total}$ = \$0.123/kWh, which is slightly higher than the 200 kWh PCM + 4 PVT configuration (\$0.1143/kWh), owing to reduced grid reliance and better use of renewable heat in the hybrid. Overall, both cost perspectives (LCOH and $LCOE_{total}$) support the same conclusion: balanced PCM sizing combined with a moderate number of PVT modules provides the most favorable techno-economic performance.

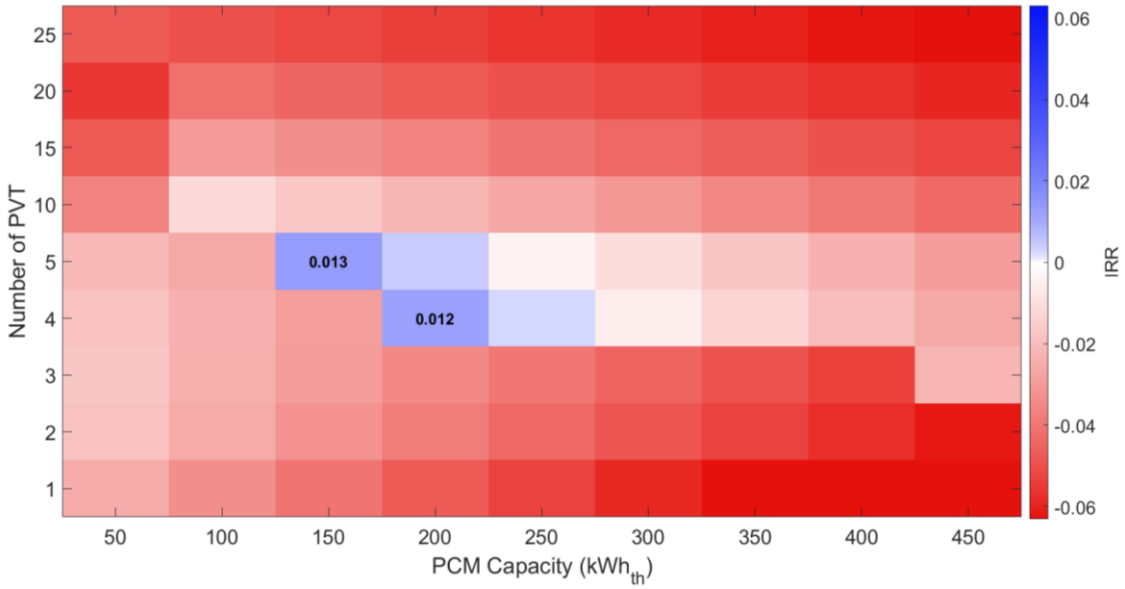

Figure 16. Internal rate of return (IRR) as a function of PCM capacity and number of PVT modules.

In the Figure 16, The IRR is negative in most combinations; only configurations with PCM capacities of 150–200 kWh and number of PVTs show positive IRR values (e.g., 0.012–0.013 ≈ 1.2–1.3%). At very low PCM capacity, grid dependency increases due to insufficient storage, and the IRR decreases; at very high PVT numbers or excessive PCMs, increasing capital costs and decreasing marginal savings push the IRR back into the negative. This pattern is consistent with the $LCOE_{total}$ surface in Figure 15. Consequently, the best economic range is for medium PCM (150–250 kWh) and a band of 3–5 PVTs; configurations beyond this range weaken the return on investment.

Across Figures 13–16, all metrics converge on the same optimum: 200 kWh PCM capacity with 4 PVT modules with 21.52 payback period (see Appendix C). This configuration equilibrates storage adequacy and financial expenditure, minimizing $LCOH$ and $LCOE_{total}$ while producing the most favorable (and marginally positive) IRR, attributable to diminished grid reliance and effective renewable thermal resource utilization

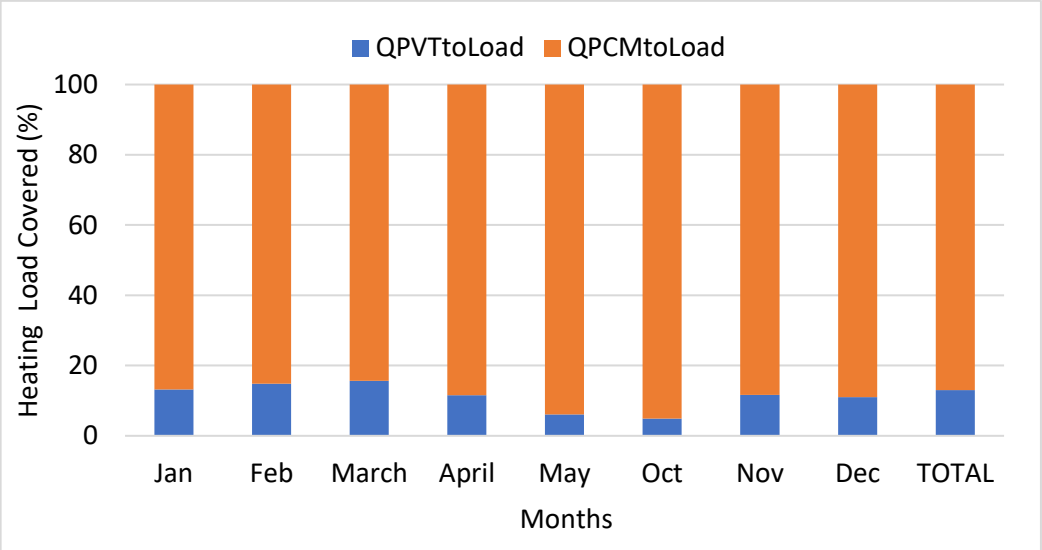

Figure 17. Heating Load Covered Ratio for Optimum Scenario

For analyzing operating characteristic of the best configuration, the share of PVT, and PCM for the heating load, the share of PVT and grid for the electricity load and the relative distribution of PVT electricity between grid and load were investigated. Figure 17 indicates the heat coverage ratio of PVT and PCM. As seen in Figure 17, for the optimal scenario (200 kWh PCM-4PVT), approximately 85–95% of the heat load is met by the PCM, and 5–15% directly by the PVT. The PVT contribution is relatively lower in April, May, and October, primarily because heat demand is lower in these months compared to other months. In the annual total, the PVT share is ≈13%, and the PCM share is ≈87%.

Similar to heat load coverage, PVT's share of the electricity load also remain low. As shown in the Figure 18, the PVT share of building electricity load coverage is approximately 18–22% in winter.

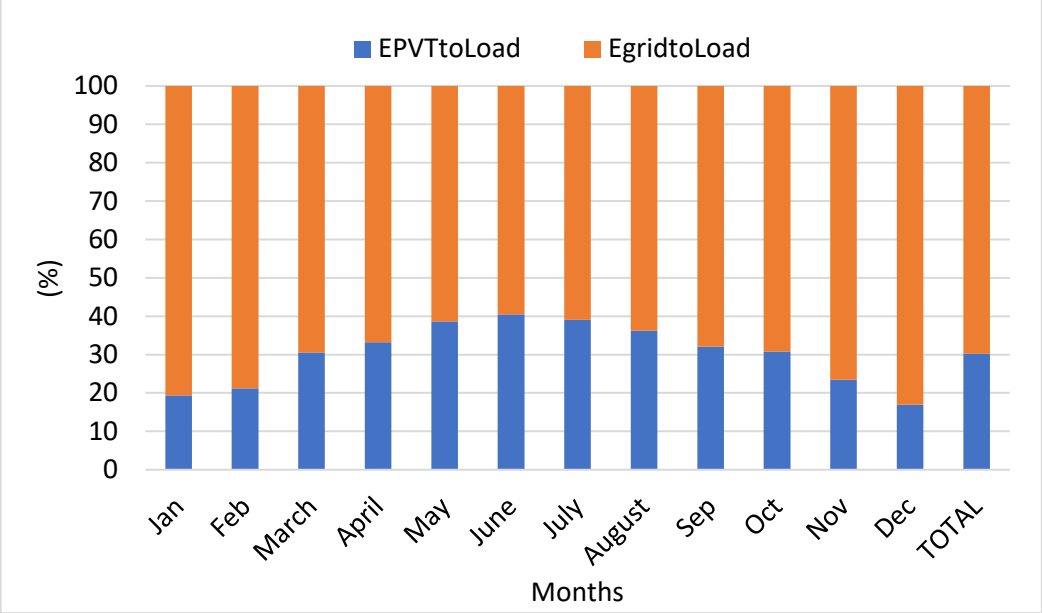

Figure 18. Electricity Load Covered Ratio for Optimum Scenario

However, with increasing irradiance, this figure rises to around 35–42% during the spring and summer. Conversely, the grid's share decreases to 60–65% during this period, rising to 78–82% in winter. Overall, PVT contributes to 30% of the annual total, while the grid contributes 70%. This pattern shows that, although the monthly electricity load remains relatively constant, the seasonality of PV generation is important, and grid dependency decreases significantly in summer.

Figure 19 visualizes how the PVT system's electricity is split each month between on-site use and export to the grid. Given the relatively flat household demand, the chart highlights that self-consumption remains modest while most production is fed into the grid.

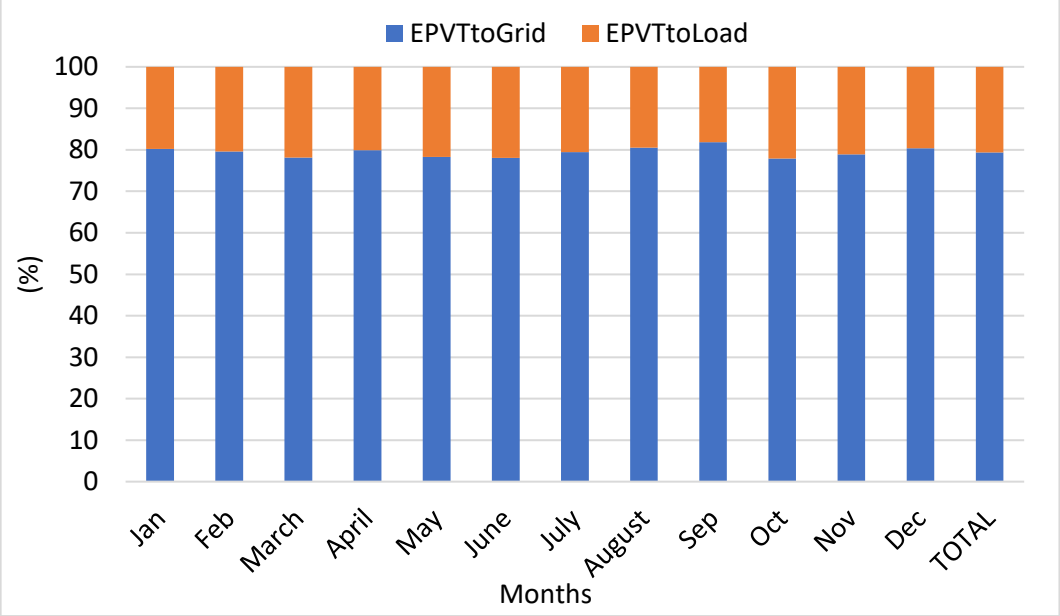

Figure 19. Monthly distribution of PVT electricity between self-consumption and grid

As seen in the Heating and Electricity loads by month graph (see Appendix A), electricity load is relatively constant throughout the year, around 170–190 kWh/month. Based on this load profile, the share of PVT generation going to self-consumption is limited throughout the year ($E_{PVTtoLoad}$ ≈ 15–22%), while the remaining portion is exported to the grid ($E_{PVTtoGrid}$ ≈ 78–85%), resulting in a total annual self-consumption of approximately 20% and export of 80%. Since the system does not contain batteries, hourly synchronization is applied; any excess PV that cannot be consumed within the same hour is fed directly to the grid.

5.5 Sensitivity Analysis

In this section, the performance of the HYB (hybrid system) (PVT–PCM–HP) system relative to the heat pump-only system is examined around the optimal design point (200 kWh PCM capacity - 4 PVTs) using a parametric sensitivity approach. The aim is to numerically demonstrate the direction and extent to which changes in key economic

inputs (i) PVT unit cost, (ii) PCM cost ($/kWh), (iii) grid electricity cost (p_{buy}) and (iv) feed-in sales price affect the hybrid system's cost metrics. For this purpose, the baseline value for each parameter was scaled between 0.5× and 2.0×, and the same market condition was applied simultaneously to both HYB and HP-only. In each case, the energy balance was established based on 8760-hour load/generation profiles; results are reported in the form of relative difference for $LCOH$, $LCOE_{el}$, $LCOE_{total}$ and IRR, Δ= (HYB – HP-only)/HP-only, in %.

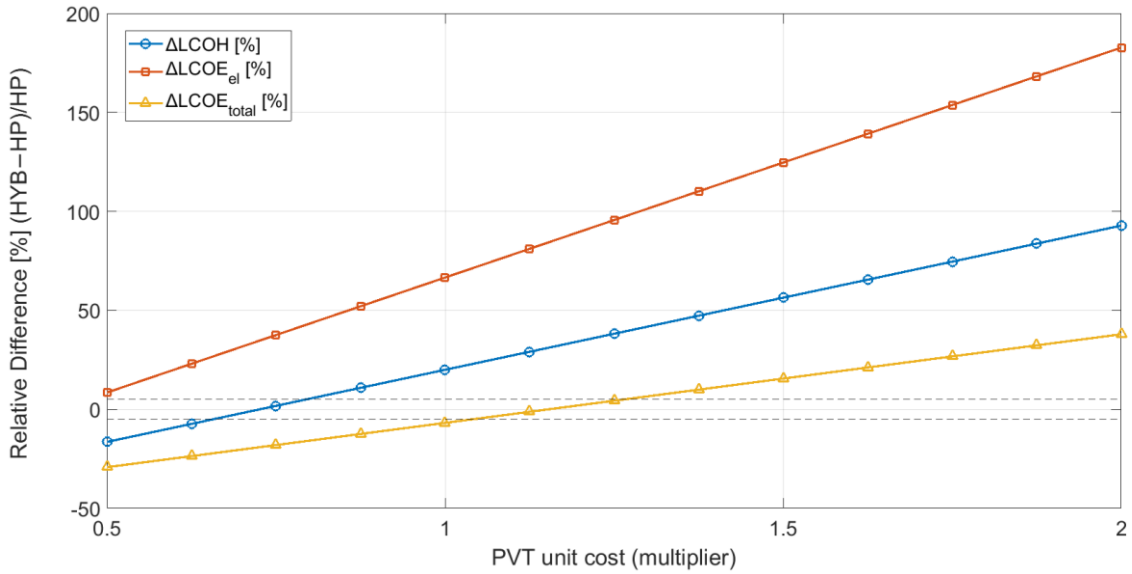

Figure 20. Sensitivity to PVT Unit CAPEX

Figure 20 indicates that, as the PVT module unit-cost multiplier increases (0.5×–2×), the relative cost difference (HYB−HP)/HP) rises linearly. In this sensitivity analysis, the ΔLCOE$_{el}$ shows the steepest slope and remains positive across the range—i.e., it does not reach parity within 0.5×–2× revealing the highest sensitivity to PVT cost. The heating metric ΔLCOH is negative at low costs and crosses zero around 0.63–0.67×, becoming positive as the multiplier approaches 1×. The ΔLCOE$_{total}$ has the smallest slope and reaches parity near 0.90–0.95×, turning unfavorable for the hybrid option at ≥1×. Overall, the sensitivity ranking is ΔLCOE$_{el}$ > $\Delta LCOH$ > ΔLCOE$_{total}$; thus, the main result is that the hybrid system's economic advantage is governed primarily by the PVT unit cost: modest cost reductions suffice for parity in ΔLCOE$_{total}$, whereas substantially larger reductions would be needed to improve the electric-service LCOE.

Figure 21 summarizes the sensitivity of the economic metrics to the PCM specific cost, reporting the hybrid system's relative differences versus the HP-only baseline across 0.5×–2× cost multipliers and highlighting parity points.

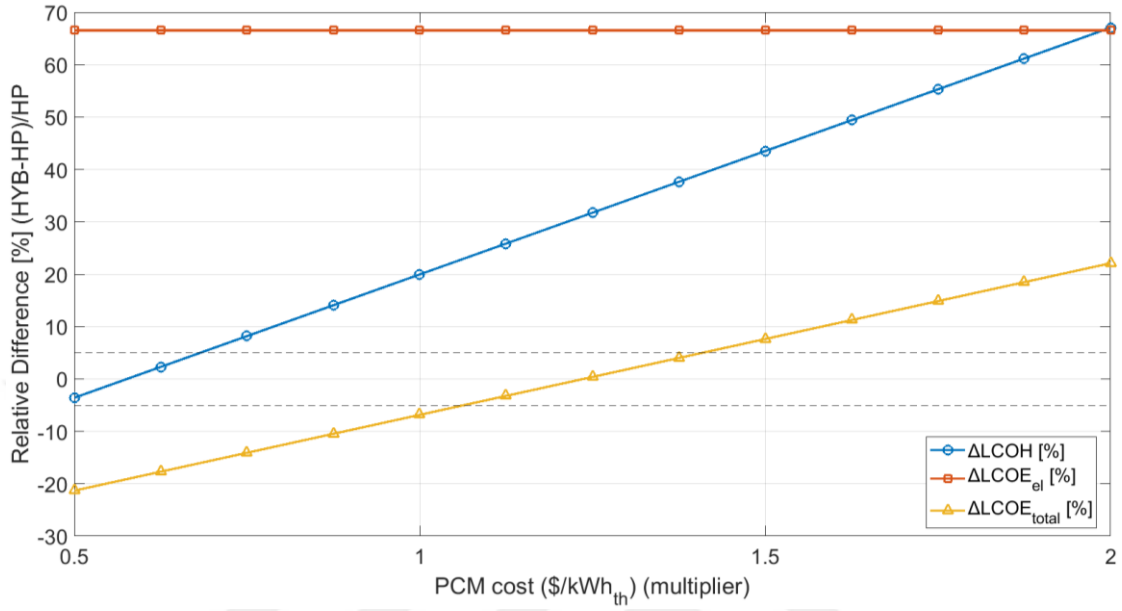

Figure 21. Sensitivity to PCM Cost

Figure 21 summarizes the sensitivity to the PCM specific-cost multiplier (0.5x–2x). ΔLCOH increases roughly linearly with the multiplier and crosses parity at ≈0.85–0.90x; it becomes positive as the multiplier approaches and exceeds 1×. $\Delta\text{LCOE}_{total}$ has a gentler slope, reaching parity at ≈1.3–1.4x—hence the hybrid retains a total-cost advantage for multipliers below this level. By contrast, ΔLCOE_{el} is nearly flat (≈66% throughout), indicating minimal sensitivity to PCM cost. Main takeaway: PCM cost primarily drives heating and overall economics; keeping PCM cost at or below ~1.0–1.3x sustains parity or advantage, while the electric-service LCOE is largely unaffected.

Figure 22 reports the sensitivity of the hybrid system to the grid-electricity purchase price. It lists the relative differences ($\Delta LCOH$, $\Delta LCOE_{el}$, $\Delta\text{LCOE}_{total}$) versus the HP-only baseline across 0.6×–2× multipliers with the feed-in tariff held constant.

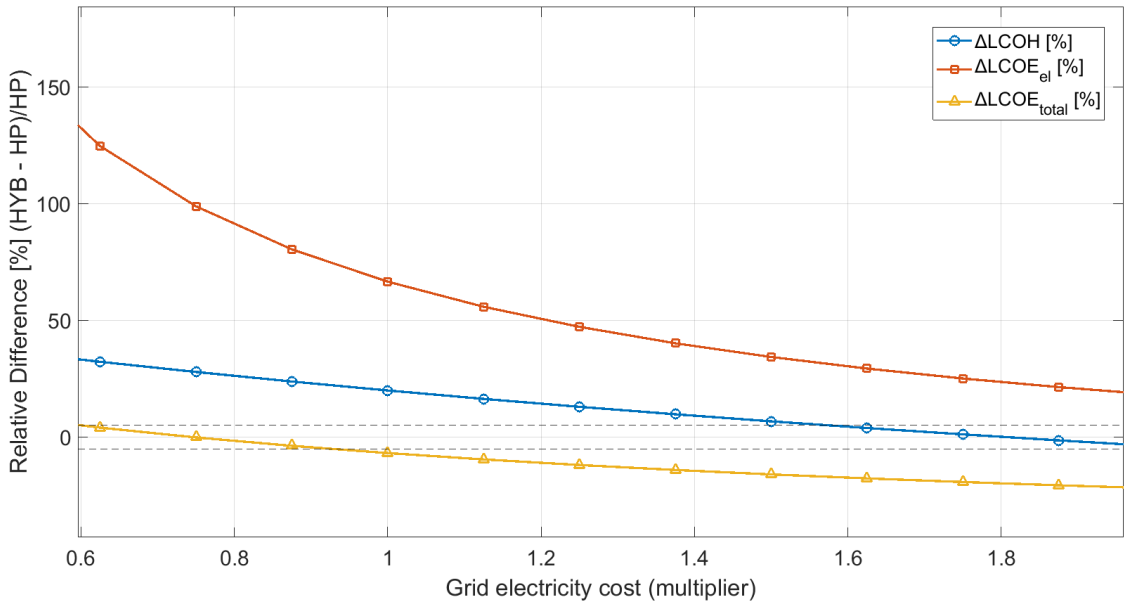

Figure 22. Sensitivity to Grid-Electricity Price (p_{buy})

Figure 22 assesses sensitivity to the grid-electricity price, modeled as a multiplier applied to the baseline p_{buy}=0.066 \$/kWh the feed-in tariff is held constant. As multipliers rise from 0.6x to 2x, the relative difference declines with a concave profile because the grid-dependent HP-only option experiences a faster increase in relative cost burden at low-to-mid price increments. $\Delta LCOE_{el}$ shows the greatest sensitivity yet remains >0 throughout; $\Delta\text{LCOE}_{\text{total}}$ crosses zero at ~0.95–1.05x and $\Delta LCOH$ reaches parity at ~1.7–1.9x. Overall, higher grid prices strengthen the hybrid's total cost advantage, while the electric-service metric remains in favour of HP-only over the examined range.

Figure 23 illustrates how the hybrid system's economics respond to changes in the grid-export (feed-in) price. The curves for ΔLCOH, ΔLCOE_el and ΔLCOE_total across 0.5–2.0× reveal the parity points and whether the advantage shifts toward the hybrid or HP-only case.

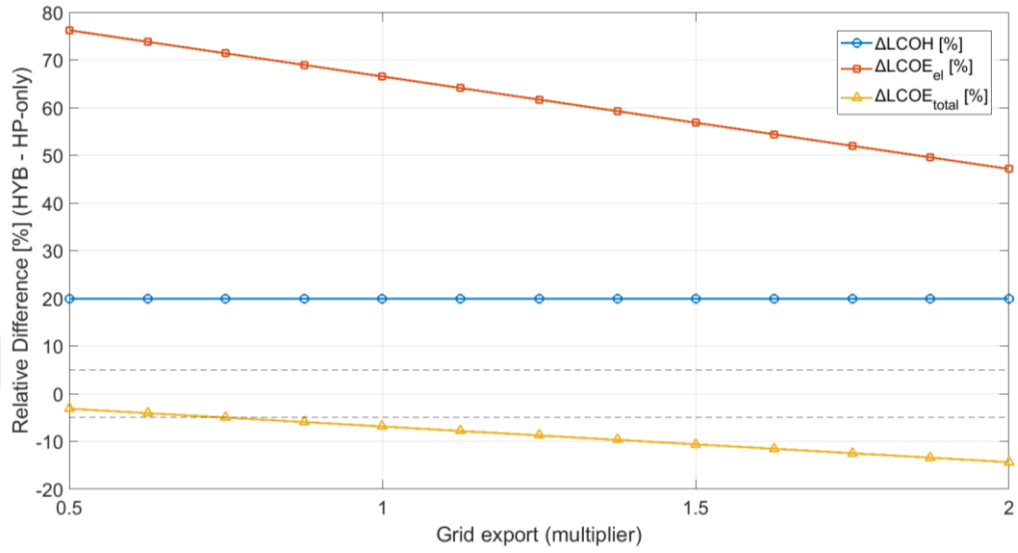

Figure 23. Sensitivity to Grid export (p_{sell})

Figure 23 shows the sensitivity of the grid electricity sales price. As the multiplier increases from 0.5 to 2.0, $\Delta LCOE_{el}$ shows the highest sensitivity but remains consistently positive, indicating that the HP-only case maintains lower electricity service costs. $\Delta LCOE_{total}$ gradually decreases and crosses the equality line around 1.0, highlighting a shift in cost competitiveness in favour of the hybrid system. In contrast, $\Delta LCOH$ remains nearly constant and approaches equality only at higher multipliers (~1.7–1.9), confirming that the hybrid configuration becomes more advantageous under upgraded grid conditions.

CHAPTER 6

CONCLUSION

6.1 Summary of Findings

This thesis examined the integration of heat pumps (HP), photovoltaic-thermal (PVT) collectors, and phase-change material (PCM)-based thermal energy storage (TES) to meet the heating and electricity needs of a residential building in İzmir's climate. Three different scenarios were modelled and evaluated technologically and economically. Main results are listed below:

- According to the findings, in the heat pump-only scenario, the system was 100% grid-dependent, the IRR was negative, and the LCOH was more than twice the price of natural gas. This demonstrates that heat pump-only structures are not economically sustainable.
- With PVT integration (Scenario 2), grid electricity consumption decreased by 16–35% between the number of PVTs 1 and 25, but the majority of the heat demand was still met by the heat pump. While a significant improvement was achieved on the electricity side, the economic return remained negative.
- With PVT + PCM integration (Scenario 3), system performance increased significantly. In the optimal configuration with a 200 kWh PCM capacity and four PVT modules, the entire heat load was met by PVT and TES, independent of the grid. In this case, the LCOH was reduced to the lowest level (≈0.091 $/kWh), with an IRR of 1.2% and a PP of 21.52 years.
- Additional sensitivity analyses revealed that system performance is highly dependent on PVT and PCM costs, as well as electricity prices. When the PVT cost was reduced by 30%, the system's LCOH decreased by approximately 12%. This demonstrates that lower panel prices directly increase the economic viability of hybrid structures.

- When the PCM cost was reduced by 50%, the IRR increased from negative to positive (+2.1%). This finding demonstrates the critical role storage costs play in economic stability.
- A 20% increase in the electricity purchase price increased the LCOH advantage of the hybrid system compared to the grid by approximately 15%. In other words, the increase in electricity prices made the hybrid system more competitive. In contrast, the low electricity sales price to the grid ($0.011/kWh) limited the economic contribution of excess electricity generated and did not significantly affect the total payback period. The results revealed that PCM integration, in particular, eliminated the heat production-consumption mismatch and made a significant economic difference.
- When analyzing the impact of PCM capacity, it was found that small storage capacities were insufficient, while excessively high capacities increased investment costs and reduced efficiency. Medium-sized PCM capacities (150–250 kWh) were determined to be the most suitable solution.

In general, the hybrid PVT–HP–PCM system provides higher energy efficiency and lower unit costs than a heat pump alone or a PVT–HP combination. These findings demonstrate that renewable energy-supported hybrid heating systems offer a viable and sustainable alternative in Mediterranean climates.

6.2 Future Works

This thesis documents the performance of photovoltaic-thermal (PVT) collectors, heat pumps (HP), and phase-change material (PCM) storage in a residential heating setting. It delivers a comparative techno-economic performance assessment and outlines directions for future research to enhance the system's applicability. Directions for future research are as follows:

- Extend the study beyond İzmir and test the PVT–HP–PCM configuration across contrasting climate zones, reflecting differences in solar resource, ambient temperature, and wind. A credible feasibility judgement requires coupling the analysis with local economic conditions—electricity tariffs, incentive schemes,

and the applicable policy framework Vary the PVT loop mass flow in response to irradiance, ambient conditions, and thermal load demand.

- Model the heat-transfer coefficients as time-varying functions of wind speed, fluid properties, flow regime, and surface temperatures, rather than treating them as constants.
- Broaden the ideal-storage assumption by explicitly modeling tank geometry, heat-exchanger area, insulation and standby losses, and PCM behavior (charge/decharge). Compare candidate PCM materials and select options suited to the climate and the chosen integration strategy.
- Implement a dynamic heat-pump COP model that captures part-load operation and variable source/sink temperatures (including defrost where relevant).
- Validate the configuration experimentally and strengthen control, by building and instrumenting a prototype, testing advanced tank designs, and developing control algorithms that coordinate PCM charge/discharge to optimize performance and reliability under real operating conditions.

REFERENCES

Arnesson, Hugo, Andreas V. Olympios, Asmaa A. Harraz, and Jingyuan Xu. 2025. "Comprehensive Energy, Economic, and Environmental Analysis of a Hybrid Photovoltaic–Thermal (PVT) Heat Pump System." *Energy* 331 (September): Article 136563. https://doi.org/10.1016/j.energy.2025.136563.

Asaee, S. Rasoul, V. Ismet Ugursal, and Ian Beausoleil-Morrison. 2017. "Techno-Economic Assessment of Solar Assisted Heat Pump System Retrofit in the Canadian Housing Stock." *Applied Energy* 190 (March): 439–52. https://doi.org/10.1016/j.apenergy.2016.12.053.

Babu, Prakash K., Amarkarthik Arunachalam, Subramaniyan Chinnasamy, and Chandrasekaran Manimuthu. 2024. "Energy-Based Techno-Economic and Environmental Feasibility Study on PV/T and PV/T Heat Pump System with Phase Change Material—A Numerical Comparative Study." *Environmental Science and Pollution Research* 31, no. 10 (March): 15627–47. https://doi.org/10.1007/s11356-024-32034-5.

Bae, Sangmu, Soowon Chae, and Yujin Nam. 2022. "Performance Analysis of Integrated Photovoltaic–Thermal and Air Source Heat Pump System through Energy Simulation." *Energies* 15, no. 2 (January): Article 528. https://doi.org/10.3390/en15020528.

Bay, Rachael A., Noah Rose, Rowan Barrett, Louis Bernatchez, Cameron K. Ghalambor, Jesse R. Lasky, Rachel B. Brem, Stephen R. Palumbi, and Peter Ralph. 2017. "Predicting Responses to Contemporary Environmental Change Using Evolutionary Response Architectures." *American Naturalist* 189, no. 5 (May): 463–73. https://doi.org/10.1086/691233.

Bayraktar, Fatih Selim, and Ramazan Köse. 2022. “Phase Change Materials: Types, Properties and Applications in Buildings.” *Kırklareli Üniversitesi Mühendislik ve Fen Bilimleri Dergisi* 8, no. 1 (April): 190–210. https://doi.org/10.34186/klujes.1126167.

Belmonte, J. F., M. Díaz-Heras, J. A. Almendros-Ibáñez, and Luisa F. Cabeza. 2022. “Simulated Performance of a Solar-Assisted Heat Pump System Including a Phase-Change Storage Tank for Residential Heating Applications: A Case Study in Madrid, Spain.” *Journal of Energy Storage* 47 (March): Article 103615. https://doi.org/10.1016/j.est.2021.103615.

Bilir, Levent, and Nurdan Yildirim. 2018. “Modeling and Performance Analysis of a Hybrid System for a Residential Application.” *Energy* 163 (November): 555–69. https://doi.org/10.1016/j.energy.2018.08.089.

Bisengimana, Emmanuel, Jinzhi Zhou, Maxime Binama, Gaudence Nyiranzeyimana, and Yanping Yuan. 2023. “Numerical Investigation of PVT Coverage on an Integrated Building–Solar–Heat Pump System: Technical and Economic Study.” *Solar Energy* 249 (January): 507–20. https://doi.org/10.1016/j.solener.2022.12.005.

Cabeza, L. F., A. Castell, C. Barreneche, A. de Gracia, and A. I. Fernández. 2011. “Materials Used as PCM in Thermal Energy Storage in Buildings: A Review.” *Renewable and Sustainable Energy Reviews* 15, no. 3 (April): 1675–95. https://doi.org/10.1016/j.rser.2010.11.018.

Chae, Soowon, Sangmu Bae, and Yujin Nam. 2023. “Economic and Environmental Analysis of the Optimum Design for the Integrated System with Air Source Heat Pump and PVT.” *Case Studies in Thermal Engineering* 48 (August): Article 103142. https://doi.org/10.1016/j.csite.2023.103142.

Dimassi, Narjes, Anouar Wajdi Dahmouni, and Med Mehdi Oueslati. 2025. “Energy Efficiency and Economic Impacts of Integrating PCM Trombe Walls in Buildings: A Multi-Climate Analysis.” *Arabian Journal for Science and Engineering* (June): online first. https://doi.org/10.1007/s13369-025-10305-8.

Duffie, John A., William A. Beckman, and Nathan Blair. 2020. *Solar Engineering of Thermal Processes, Photovoltaics and Wind*. 5th ed. Hoboken, NJ: Wiley. https://doi.org/10.1002/9781119540328.

Fiorentini, Massimo, Paul Cooper, and Zhenjun Ma. 2015. “Development and Optimization of an Innovative HVAC System with Integrated PVT and PCM Thermal Storage for a Net-Zero Energy Retrofitted House.” *Energy and Buildings* 94 (May): 21–32. https://doi.org/10.1016/j.enbuild.2015.02.018.

Gagliano, Antonio, Giuseppe Marco Tina, and Stefano Aneli. 2025. “Improvement in Energy Self-Sufficiency in Residential Buildings Using Photovoltaic Thermal Plants, Heat Pumps, and Electrical and Thermal Storage.” *Energies* 18, no. 5 (March): 1159. https://doi.org/10.3390/en18051159.

Gao, Jinshuang, Sheng Li, M. Adnouni, Huang Yan, Meng Yu, Yazhou Zhao, and Xuejun Zhang. 2024. “Simulation Study on Thermal Performance of Solar Coupled Air Source Heat Pump System with Phase Change Heat Storage in Cold Regions.” *Energy* 308 (November): Article 132921. https://doi.org/10.1016/j.energy.2024.132921.

Giama, Effrosyni, Konstantinos Sittas, Georgios Chantzis, and Agis Papadopoulos. 2025. “Carbon Neutrality in the Building Sector: Optimization of Heat Pumps Operation in Combination to PV/T as Auxiliary Renewable Energy System.” *Energy* 330 (September): Article 136726. https://doi.org/10.1016/j.energy.2025.136726.

Grazer, Brian, and Charles Fishman. 2015. *A Curious Mind: The Secret to a Bigger Life*. New York: Simon & Schuster.

Herrando, M., A. Coca-Ortegón, I. Guedea, and N. Fueyo. 2023. "Experimental Validation of a Solar System Based on Hybrid Photovoltaic–Thermal Collectors and a Reversible Heat Pump for the Energy Provision in Non-Residential Buildings." *Renewable and Sustainable Energy Reviews* 178 (May): Article 113233. https://doi.org/10.1016/j.rser.2023.113233.

Hirschey, Jason, Kyle R. Gluesenkamp, Anne Mallow, and Samuel Graham. 2018. "Review of Inorganic Salt Hydrates with Phase Change Temperature in Range of 5°C to 60°C and Material Cost Comparison with Common Waxes." In *Proceedings of the 5th International High Performance Buildings Conference at Purdue*, West Lafayette, IN, July 9–12, Paper 1–10.

IPCC. 2023. *Climate Change 2023: Synthesis Report*. Geneva: Intergovernmental Panel on Climate Change. https://doi.org/10.59327/IPCC/AR6-9789291691647.

Kaygusuz, K., and T. Ayhan. 1999. "Experimental and Theoretical Investigation of Combined Solar Heat Pump System for Residential Heating." *Energy Conversion and Management* 40, no. 13 (September): 1377–96. https://doi.org/10.1016/S0196-8904(99)00026-6.

Keng, Shao-Hsun, Chun-Hung Lin, and Peter F. Orazem. 2017. "Expanding College Access in Taiwan, 1978–2014: Effects on Graduate Quality and Income Inequality." *Journal of Human Capital* 11, no. 1 (Spring): 1–34. https://doi.org/10.1086/690235.

Kul, Onder, and Mehmet Nurettin Uğural. 2022. "Comparative Economic and Experimental Assessment of Air Source Heat Pump and Gas-Fired Boiler: A Case

Study from Turkey." *Sustainability* 14, no. 21 (November): Article 14298. https://doi.org/10.3390/su142114298.

LaSalle, Peter. 2017. "Conundrum: A Story about Reading." *New England Review* 38 (1): 95–109.

Li, Jinping, Chaofan Qu, Caijun Li, Xiaomin Liu, and Vojislav Novakovic. 2022. "Technical and Economic Performance Analysis of Large Flat Plate Solar Collector Coupled Air Source Heat Pump Heating System." *Energy and Buildings* 277 (December): Article 112564. https://doi.org/10.1016/j.enbuild.2022.112564.

Li, Master Yalun, Baoguo Li, Caiyun Liu, Shuqiang Su, Honghai Xiao, and Chuanhui Zhu. 2020. "Design and Experimental Investigation of a Phase Change Energy Storage Air-Type Solar Heat Pump Heating System." *Applied Thermal Engineering* 179 (October): Article 115506. https://doi.org/10.1016/j.applthermaleng.2020.115506.

Liu, Wenjie, Jian Yao, Teng Jia, Yao Zhao, Yanjun Dai, Junjie Zhu, and Vojislav Novakovic. 2023. "The Performance Optimization of DX-PVT Heat Pump System for Residential Heating." *Renewable Energy* 206 (April): 1106–19. https://doi.org/10.1016/j.renene.2023.02.089.

Mouzeviris, Georgios A., and Konstantinos T. Papakostas. 2022. "Study on Air-to-Water Heat Pumps Seasonal Performances for Heating in Greece." *Energies* 15, no. 1 (January): Article 279. https://doi.org/10.3390/en15010279.

Nair, Ajay Muraleedharan, Christopher Wilson, Ming Jun Huang, Philip Griffiths, and Neil Hewitt. 2022. "Phase Change Materials in Building Integrated Space Heating and Domestic Hot Water Applications: A Review." *Journal of Energy Storage* 55 (May): Article 105227. https://doi.org/10.1016/j.est.2022.105227.

Obalanlege, Mustapha A., Yasser Mahmoudi, Roy Douglas, Ehsan Ebrahimnia-Bajestan, John Davidson, and David Bailie. 2020. “Performance Assessment of a Hybrid Photovoltaic–Thermal and Heat Pump System for Solar Heating and Electricity.” *Renewable Energy* 148 (April): 558–72. https://doi.org/10.1016/j.renene.2019.10.061.

Obalanlege, Mustapha A., Jingyuan Xu, Christos N. Markides, and Yasser Mahmoudi. 2022. “Techno-Economic Analysis of a Hybrid Photovoltaic–Thermal Solar-Assisted Heat Pump System for Domestic Hot Water and Power Generation.” *Renewable Energy* 196 (August): 720–36. https://doi.org/10.1016/j.renene.2022.07.044.

Özçelik, Batuğhan Rüştü, Arslan Çağlayan Gürel, and Özay Akdemir. 2023. “Denizli’deki Bir Villanın Isı Pompasıyla Isıtılmasının İncelenmesi.” *Teknik Bilimler Dergisi* 13, no. 1 (April): 41–47. https://doi.org/10.35354/tbed.1177589.

Pei, Gang, Jie Ji, Ke-Liang Liu, Han-Feng He, and Ai-Guo Jiang. 2008. “Numerical Study of PV/T-SAHP System.” *Journal of Zhejiang University—Science A* 9, no. 7 (July): 970–80. https://doi.org/10.1631/jzus.A0720143.

Pereira da Cunha, Jose, and Philip Eames. 2016. “Thermal Energy Storage for Low and Medium Temperature Applications Using Phase Change Materials—A Review.” *Applied Energy* 177 (September): 227–48. https://doi.org/10.1016/j.apenergy.2016.05.097.

Plytaria, Maria T., Christos Tzivanidis, Evangelos Bellos, and Kimon A. Antonopoulos. 2018. “Energetic Investigation of Solar-Assisted Heat Pump Underfloor Heating Systems with and without Phase Change Materials.” *Energy Conversion and Management* 173 (October): 626–39. https://doi.org/10.1016/j.enconman.2018.08.010.

Plytaria, Maria T., Evangelos Bellos, Christos Tzivanidis, and Kimon A. Antonopoulos. 2019. “Financial and Energetic Evaluation of Solar-Assisted Heat Pump Underfloor Heating Systems with Phase Change Materials.” *Applied Thermal Engineering* 149 (February): 548–64. https://doi.org/10.1016/j.applthermaleng.2018.12.075.

Sarbu, Ioan, Daniel Dan, and Calin Sebarchievici. 2014. “Performances of Heat Pump Systems as Users of Renewable Energy for Building Heating/Cooling.” *WSEAS Transactions on Heat and Mass Transfer* 9: 51–62.

Shao, Suola, Huan Zhang, Xianwang Fan, Shijun You, Yaran Wang, and Shen Wei. 2021. “Thermodynamic and Economic Analysis of the Air Source Heat Pump System with Direct-Condensation Radiant Heating Panel.” *Energy* 225 (June): Article 120195. https://doi.org/10.1016/j.energy.2021.120195.

Soytürk, Gamze, Önder Kızılkan, and Mehmet Akif Ezan. 2022. “Mathematical Modeling of a Photovoltaic Thermal (PV/T) Collector.” *Uluslararası Teknolojik Bilimler Dergisi* 14, no. 3 (September): 144–52. https://doi.org/10.55974/utbd.1168551.

Teamah, H. M. 2021. “Comprehensive Review of the Application of Phase Change Materials in Residential Heating Applications.” *Alexandria Engineering Journal* 60, no. 4 (August): 3829–43. https://doi.org/10.1016/j.aej.2021.02.053.

Tiwari, Arvind, and M. S. Sodha. 2006. “Performance Evaluation of Solar PV/T System: An Experimental Validation.” *Solar Energy* 80, no. 7 (July): 751–59. https://doi.org/10.1016/j.solener.2005.07.006.

Udovichenko, Artur, and Lexuan Zhong. 2020. “Techno-Economic Analysis of Air-Source Heat Pump (ASHP) Technology for Single-Detached Home Heating

Applications in Canada." *Science and Technology for the Built Environment* 26, no. 10 (November): 1352–70. https://doi.org/10.1080/23744731.2020.1787083.

Vallati, A., P. Ocłoń, C. Colucci, L. Mauri, R. de Lieto Vollaro, and J. Taler. 2019. "Energy Analysis of a Thermal System Composed by a Heat Pump Coupled with a PVT Solar Collector." *Energy* 174 (May): 91–96. https://doi.org/10.1016/j.energy.2019.02.152.

Wang, Gang, Yaohua Zhao, Zhenhua Quan, and Jiannan Tong. 2018. "Application of a Multi-Function Solar–Heat Pump System in Residential Buildings." *Applied Thermal Engineering* 130 (February): 922–37. https://doi.org/10.1016/j.applthermaleng.2017.10.046.

Wang, Yubo, Zhenhua Quan, Yaohua Zhao, Lincheng Wang, and Zichu Liu. 2022. "Performance and Optimization of a Novel Solar–Air Source Heat Pump Building Energy Supply System with Energy Storage." *Applied Energy* 324 (October): Article 119706. https://doi.org/10.1016/j.apenergy.2022.119706.

Wang, Zheng, Mark B. Luther, Mehdi Amirkhani, Chunlu Liu, and Peter Horan. 2021. "State of the Art on Heat Pumps for Residential Buildings." *Buildings* 11, no. 8 (August): Article 360. https://doi.org/10.3390/buildings11080350.

Wijesuriya, Sajith, Matthew Brandt, and Paulo Cesar Tabares-Velasco. 2018. "Parametric Analysis of a Residential Building with Phase Change Material (PCM)-Enhanced Drywall, Precooling, and Variable Electric Rates in a Hot and Dry Climate." *Applied Energy* 222 (July): 497–514. https://doi.org/10.1016/j.apenergy.2018.03.119.

Wu, Jianghong, Ting Xian, and Xuan Liu. 2019. "All-Weather Characteristic Studies of a Direct Expansion Solar Integrated Air Source Heat Pump System Based on

PCMs.” *Solar Energy* 191 (October): 34–45. https://doi.org/10.1016/j.solener.2019.08.057.

Yang, Tianrun, Wen Liu, Gert Jan Kramer, and Qie Sun. 2021. “Seasonal Thermal Energy Storage: A Techno-Economic Literature Review.” *Renewable and Sustainable Energy Reviews* 148 (April): Article 110732. https://doi.org/10.1016/j.rser.2021.110732.

Yao, Jian, Hui Xu, Yanjun Dai, and Mingjun Huang. 2020. “Performance Analysis of Solar Assisted Heat Pump Coupled with Built-in PCM Heat Storage Based on PV/T Panel.” *Solar Energy* 197 (February): 279–91. https://doi.org/10.1016/j.solener.2020.01.002.

Zhao, Yuan, Jun Gao, Bo Zhu, Tang Qian, Dabiao Wang, Qilong Wang, Ruirui Zhao, and Baomin Dai. 2023. “Energy Conservation and Carbon Reduction of Air Source Heat Pump for District Heating.” *Journal of Physics: Conference Series* 2463 (July): Article 012067. https://doi.org/10.1088/1742-6596/2463/1/012067.

APPENDIX A

HEATING AND ELECTRICITY DEMAND OF HOUSE

Bilir and Yıldırım (2018) calculated the total annual heating load and electricity load of a 117 m² residential building in Izmir as 3037 kWh and 2183 kWh, respectively. These values were used as reference inputs for the performance evaluation of the systems studied in this thesis.

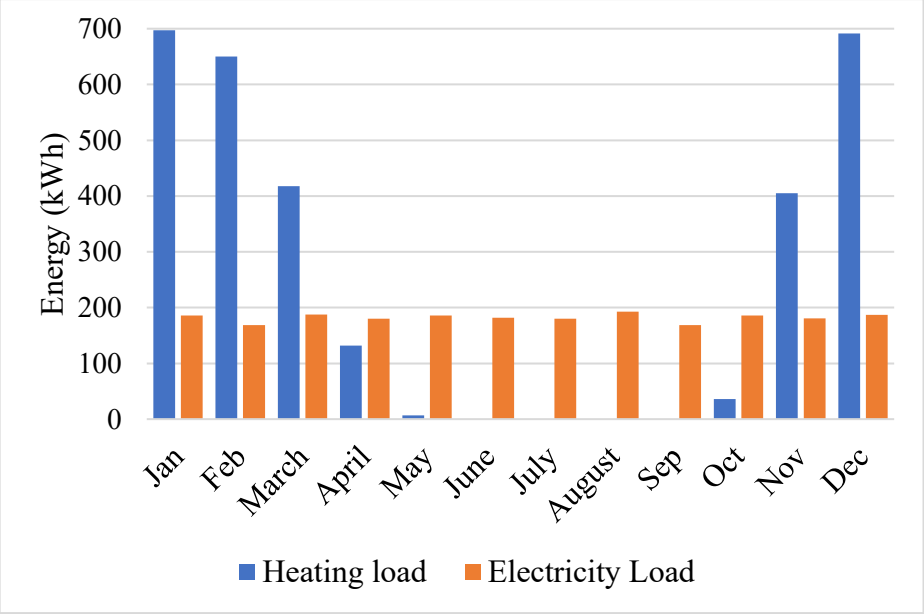

Figure 24. Heating and Electricity loads by months (Bilir and Yildirim 2018)

As illustrated in Figure 24, the monthly distribution of heating and electricity consumption. Heating demand is higher in winter (January, February, December) and declines to almost zero in summer. The electricity demand is constant throughout the year due to the daily dependence on hot water, appliances and lighting factors, while heating demand is variable due to seasonal fluctuations.

APPENDIX B

ENERGY RESULTS FOR ALL SCENARIOS

Table .10 Energy Results of Scenerio 1 - 2

C_{PCM}	N_{PVT}	Q_{PVT}	$Q_{PVTto\ load}$	$Q_{PCMto\ load}$	Q_{HP}	E_{PVT}	$E_{PVTto\ load}$	$E_{PVTto\ grid}$	E_{HP}	$E_{gridto\ load}$
0	0	0	0	0	3036.69	0	0	0	867.62	3063.89
0	1	2971.44	262.00	0	2774.68	804.85	391.78	413.07	792.77	2597.25
0	2	5942.87	335.24	0	2701.44	1609.70	508.44	1101.26	771.84	2459.66
0	3	8914.31	372.35	0	2664.33	2414.55	589.83	1824.71	761.24	2367.67
0	4	11885.75	394.31	0	2642.38	3219.40	664.42	2554.97	754.97	2286.80
0	5	14857.18	408.34	0	2628.34	4024.25	732.56	3291.68	750.95	2214.65
0	10	29714.37	445.44	0	2591.24	8048.49	897.89	7150.60	740.35	2038.72
0	15	44571.55	466.14	0	2570.55	12072.74	975.60	11097.13	734.44	1955.10
0	20	59428.74	480.87	0	2555.81	16096.98	1023.26	15073.72	730.23	1903.24
0	25	74285.92	492.71	0	2543.97	20121.23	1056.18	19065.05	726.85	1866.93

Table 11. Energy Results of Scenerio 3 for C_{PCM}= 50 (kWh)

C_{PCM}	N_{PVT}	Q_{PVT}	$Q_{PVTtoload}$	$Q_{PCMtoload}$	Q_{HP}	E_{PVT}	$E_{PVTtoload}$	$E_{PVTtogrid}$	E_{HP}	$E_{gridtoload}$
50	0	0	0	50	2986.69	0	0	0	853.34	3049.60
50	1	2971.44	262.00	841.12	1933.57	804.85	388.70	416.15	552.45	2360.01
50	2	5942.87	335.24	1532.21	1169.23	1609.70	506.56	1103.14	334.07	2023.77
50	3	8914.31	372.35	2005.55	658.78	2414.55	588.37	1826.18	188.22	1796.11
50	4	11885.75	394.31	2338.27	304.11	3219.40	663.70	2555.69	86.89	1619.45
50	5	14857.18	408.34	2456.73	171.61	4024.25	732.05	3292.20	49.03	1513.24
50	10	29714.37	445.44	2564.03	27.21	8048.49	897.43	7151.06	7.77	1306.61
50	15	44571.55	466.14	2564.95	5.60	12072.74	975.40	11097.34	1.60	1222.46
50	20	59428.74	480.87	2553.76	2.05	16096.98	1023.20	15073.78	0.59	1173.65
50	25	74285.92	492.71	2543.97	0	20121.23	1056.14	19065.09	0	1140.12

Table 12. Energy Results of Scenerio 3 for C_{PCM}= 50 (kWh)

C_{PCM}	N_{PVT}	Q_{PVT}	$Q_{PVTtoload}$	$Q_{PCMtoload}$	Q_{HP}	E_{PVT}	$E_{PVTtoload}$	$E_{PVTtogrid}$	E_{HP}	$E_{gridtoload}$
100	0	0	0	100.00	2936.69	0	0	0	839.05	3035.31
100	1	2971.44	262.00	941.12	1833.57	804.85	388.70	416.15	523.88	2331.44
100	2	5942.87	335.24	1635.67	1065.78	1609.70	506.56	1103.14	304.51	1994.21
100	3	8914.31	372.35	2121.70	542.64	2414.55	588.36	1826.19	155.04	1762.94
100	4	11885.75	394.31	2503.50	138.88	3219.40	663.70	2555.69	39.68	1572.24
100	5	14857.18	408.34	2596.21	32.13	4024.25	732.05	3292.20	9.18	1473.39
100	10	29714.37	445.44	2591.24	0	8048.49	897.43	7151.06	0	1298.83
100	15	44571.55	466.14	2570.55	0	12072.74	975.40	11097.34	0	1220.86
100	20	59428.74	480.87	2555.81	0	16096.98	1023.20	15073.78	0	1173.06
100	25	74285.92	492.71	2543.97	0	20121.23	1056.14	19065.09	0	1140.12

Table 13. Energy Results of Scenerio 3 for C_{PCM}= 150 (kWh)

C_{PCM}	N_{PVT}	Q_{PVT}	$Q_{PVTtoload}$	$Q_{PCMtoload}$	Q_{HP}	E_{PVT}	$E_{PVTtoload}$	$E_{PVTtogrid}$	E_{HP}	$E_{gridtoload}$
150	0	0	0	150.00	2886.69	0	0	0	824.77	3021.03
150	1	2971.44	262.00	1041.12	1733.57	804.85	388.70	416.15	495.31	2302.86
150	2	5942.87	335.24	1735.67	965.78	1609.70	506.56	1103.14	275.94	1965.64
150	3	8914.31	372.35	2221.70	442.64	2414.55	588.36	1826.19	126.47	1734.37
150	4	11885.75	394.31	2611.49	30.89	3219.40	663.70	2555.69	8.83	1541.38
150	5	14857.18	408.34	2628.34	0	4024.25	732.05	3292.20	0	1464.21
150	10	29714.37	445.44	2591.24	0	8048.49	897.43	7151.06	0	1298.83
150	15	44571.55	466.14	2570.55	0	12072.74	975.40	11097.34	0	1220.86
150	20	59428.74	480.87	2555.81	0	16096.98	1023.20	15073.78	0	1173.06
150	25	74285.92	492.71	2543.97	0	20121.23	1056.14	19065.09	0	1140.12

Table 14. Energy Results of Scenerio 3 for C_{PCM}= 150 (kWh)

C_{PCM}	N_{PVT}	Q_{PVT}	$Q_{PVTtoload}$	$Q_{PCMtoload}$	Q_{HP}	E_{PVT}	$E_{PVTtoload}$	$E_{PVTtogrid}$	E_{HP}	$E_{gridtoload}$
200	0	0	0	200.00	2836.69	0	0	0	810.48	3006.74
200	1	2971.44	262.00	1141.12	1633.57	804.85	388.70	416.15	466.73	2274.29
200	2	5942.87	335.24	1835.67	865.78	1609.70	506.55	1103.15	247.36	1937.07
200	3	8914.31	372.35	2321.70	342.64	2414.55	588.36	1826.19	97.90	1705.80
200	4	11885.75	394.31	2642.38	0	3219.40	663.70	2555.69	0	1532.56
200	5	14857.18	408.34	2628.34	0	4024.25	732.05	3292.20	0	1464.21
200	10	29714.37	445.44	2591.24	0	8048.49	897.43	7151.06	0	1298.83
200	15	44571.55	466.14	2570.55	0	12072.74	975.40	11097.34	0	1220.86
200	20	59428.74	480.87	2555.81	0	16096.98	1023.20	15073.78	0	1173.06
200	25	74285.92	492.71	2543.97	0	20121.23	1056.14	19065.09	0	1140.12

Table 15. Energy Results of Scenerio 3 for C_{PCM}= 250 (kWh)

C_{PCM}	N_{PVT}	Q_{PVT}	$Q_{PVTtoload}$	$Q_{PCMtoload}$	Q_{HP}	E_{PVT}	$E_{PVTtoload}$	$E_{PVTtogrid}$	E_{HP}	$E_{gridtoload}$
250	0	0	0	250.00	2786.69	0	0	0	796.20	2992.46
250	1	2971.44	262.00	1241.12	1533.57	804.85	388.70	416.15	438.16	2245.72
250	2	5942.87	335.24	1935.67	765.78	1609.70	506.55	1103.15	218.79	1908.50
250	3	8914.31	372.35	2421.70	242.64	2414.55	588.36	1826.19	69.32	1677.23
250	4	11885.75	394.31	2642.38	0	3219.40	663.70	2555.69	0	1532.56
250	5	14857.18	408.34	2628.34	0	4024.25	732.05	3292.20	0	1464.21
250	10	29714.37	445.44	2591.24	0	8048.49	897.43	7151.06	0	1298.83
250	15	44571.55	466.14	2570.55	0	12072.74	975.40	11097.34	0	1220.86
250	20	59428.74	480.87	2555.81	0	16096.98	1023.20	15073.78	0	1173.06
250	25	74285.92	492.71	2543.97	0	20121.23	1056.14	19065.09	0	1140.12

Table 16. Energy Results of Scenerio 3 for C_{PCM}= 300 (kWh)

C_{PCM}	N_{PVT}	Q_{PVT}	$Q_{PVTtoload}$	$Q_{PCMtoload}$	Q_{HP}	E_{PVT}	$E_{PVTtoload}$	$E_{PVTtogrid}$	E_{HP}	$E_{gridtoload}$
300	0	0	0	300.00	2736.69	0	0	0	781.91	2978.17
300	1	2971.44	262.00	1341.12	1433.57	804.85	388.64	416.21	409.59	2217.21
300	2	5942.87	335.24	2035.67	665.78	1609.70	506.55	1103.15	190.22	1879.93
300	3	8914.31	372.35	2515.47	148.86	2414.55	588.36	1826.19	42.53	1650.44
300	4	11885.75	394.31	2642.38	0	3219.40	663.70	2555.69	0	1532.56
300	5	14857.18	408.34	2628.34	0	4024.25	732.05	3292.20	0	1464.21
300	10	29714.37	445.44	2591.24	0	8048.49	897.43	7151.06	0	1298.83
300	15	44571.55	466.14	2570.55	0	12072.74	975.40	11097.34	0	1220.86
300	20	59428.74	480.87	2555.81	0	16096.98	1023.20	15073.78	0	1173.06
300	25	74285.92	492.71	2543.97	0	20121.23	1056.14	19065.09	0	1140.12

Table 17. Energy Results of Scenerio 3 for C_{PCM}= 350 (kWh)

C_{PCM}	N_{PVT}	Q_{PVT}	$Q_{PVTtoload}$	$Q_{PCMtoload}$	Q_{HP}	E_{PVT}	$E_{PVTtoload}$	$E_{PVTtogrid}$	E_{HP}	$E_{gridtoload}$
350	0	0	0	350.00	2686.69	0	0	0	767.62	2963.89
350	1	2971.44	262.00	1441.12	1333.57	804.85	388.64	416.21	381.02	2188.64
350	2	5942.87	335.24	2135.67	565.78	1609.70	506.55	1103.15	161.65	1851.36
350	3	8914.31	372.35	2565.47	98.86	2414.55	588.36	1826.19	28.25	1636.15
350	4	11885.75	394.31	2642.38	0	3219.40	663.70	2555.69	0	1532.56
350	5	14857.18	408.34	2628.34	0	4024.25	732.05	3292.20	0	1464.21
350	10	29714.37	445.44	2591.24	0	8048.49	897.43	7151.06	0	1298.83
350	15	44571.55	466.14	2570.55	0	12072.74	975.40	11097.34	0	1220.86
350	20	59428.74	480.87	2555.81	0	16096.98	1023.20	15073.78	0	1173.06
350	25	74285.92	492.71	2543.97	0	20121.23	1056.14	19065.09	0	1140.12

Table 18. Energy Results of Scenerio 3 for C_{PCM}= 400 (kWh)

C_{PCM}	N_{PVT}	Q_{PVT}	$Q_{PVTtoload}$	$Q_{PCMtoload}$	Q_{HP}	E_{PVT}	$E_{PVTtoload}$	$E_{PVTtogrid}$	E_{HP}	$E_{gridtoload}$
400	0	0	0	400.00	2636.69	0	0	0	753.34	2949.60
400	1	2971.44	262.00	1541.12	1233.57	804.85	388.64	416.21	352.45	2160.07
400	2	5942.87	335.24	2235.67	465.78	1609.70	506.55	1103.15	133.08	1822.79
400	3	8914.31	372.35	2615.47	48.86	2414.55	588.36	1826.19	13.96	1621.86
400	4	11885.75	394.31	2642.38	0	3219.40	663.70	2555.69	0	1532.56
400	5	14857.18	408.34	2628.34	0	4024.25	732.05	3292.20	0	1464.21
400	10	29714.37	445.44	2591.24	0	8048.49	897.43	7151.06	0	1298.83
400	15	44571.55	466.14	2570.55	0	12072.74	975.40	11097.34	0	1220.86
400	20	59428.74	480.87	2555.81	0	16096.98	1023.20	15073.78	0	1173.06
400	25	74285.92	492.71	2543.97	0	20121.23	1056.14	19065.09	0	1140.12

Table 19. Energy Results of Scenerio 3 for C_{PCM}= 400 (kWh)

C_{PCM}	N_{PVT}	Q_{PVT}	$Q_{PVTtoload}$	$Q_{PCMtoload}$	Q_{HP}	E_{PVT}	$E_{PVTtoload}$	$E_{PVTtogrid}$	E_{HP}	$E_{gridtoload}$
450	0	0	0	450	2586.69	0	0	0	739.05	2935.31
450	1	2971.44	262.00	1641.12	1133.57	804.85	388.63	416.22	323.88	2131.51
450	2	5942.87	335.24	2335.67	365.78	1609.70	506.55	1103.15	104.51	1794.22
450	3	8914.31	372.35	2664.33	0	2414.55	588.36	1826.19	0	1607.91
450	4	11885.75	394.31	2642.38	0	3219.40	663.70	2555.69	0	1532.56
450	5	14857.18	408.34	2628.34	0	4024.25	732.05	3292.20	0	1464.21
450	10	29714.37	445.44	2591.24	0	8048.49	897.43	7151.06	0	1298.83
450	15	44571.55	466.14	2570.55	0	12072.74	975.40	11097.34	0	1220.86
450	20	59428.74	480.87	2555.81	0	16096.98	1023.20	15073.78	0	1173.06
450	25	74285.92	492.71	2543.97	0	20121.23	1056.14	19065.09	0	1140.12